Master's thesis

NTNU
Norwegian University of Science and Technology
Faculty of Medicine and Health Sciences
Department of Clinical and Molecular Medicine

Lu Bai

Expression and function of FSTL5 in multiple myeloma cells

Master's thesis in Molecular Medicine
Supervisor: Toril Holien
Co-supervisor: Kristine Misund
May 2021

NTNU
Norwegian University of
Science and Technology

Lu Bai

Expression and function of FSTL5 in multiple myeloma cells

Master's thesis in Molecular Medicine
Supervisor: Toril Holien
Co-supervisor: Kristine Misund
May 2021

Norwegian University of Science and Technology
Faculty of Medicine and Health Sciences
Department of Clinical and Molecular Medicine

NTNU
Norwegian University of
Science and Technology

Acknowledgement

This master project was carried out at the Faculty of Medicine and Health Sciences, Department of Clinical and Molecular Medicine at the Norwegian University of Science and Technology (NTNU).

I would like to start by thanking my supervisor, Toril Holien, for teaching me how to conduct scientific research, solving my problems, and always being there to help with patience. I also want to express thanks to my co-supervisor, Kristine Misund, who has given lots of valuable ideas on the genetic part of this project.

I am also grateful for the cell lines prepared by Hanne Hella, Berit Størdal, and Glenn Buene, and for the brain organoids cDNA gift given by Dr. Wei Wang.

In the end, I want to say thanks to all the researchers, employees, and students of the myeloma group for their kind help and to my family and boyfriend for their mental support.

Trondheim, May 2021

Lu Bai

Abstract

Multiple myeloma (MM) is an incurable cancer arising in the antibody-producing plasma cells that are located in the bone marrow. The malignant cells disturb the balance between bone forming and bone degrading cells, leading to bone disease in most patients. Follistatin (FST) and its related follistatin-like (FSTL) molecules are antagonists of the transforming growth factor-β (TGF-β) family of proteins, which play important roles in the progression of MM. Recent studies showed that a member of FSTL molecules called FSTL5 was expressed in malignant myeloma cells but not in normal plasma cells and it had a prognostic value in MM. However, due to the limited knowledge of the function of FSTL5, its role in MM remains unknown. The aim of this thesis was to further explore FSTL5 expression in MM and try to learn more about its function.

The expression of FSTL5 mRNA in different cell types as well as a panel of human myeloma cell lines (HMCLs) was investigated. FSTL5 protein in HMCLs was detected by western blot using different antibodies that were raised towards different parts of the protein and FSTL5 gene knockout (KO) and knockdown (KD) strategies were applied to validate antibodies' specificity. In addition, the effect of FSTL5 KO/KD on TGF-β family members and Myc inhibitor was examined and the role of FSTL5 in caspases activities was preliminary explored.

The results demonstrated FSTL5 mRNA expression in HMCLs and the existence of a new FSTL5 transcript variant, whereas FSTL5 protein expression in HMCLs was still undetermined. An antagonizing effect of FSTL5 on BMP and activins was not detected, no effect on cell viability was seen by FSTL5 KD, and no evidence of caspases regulation of FSTL5 was found. In conclusion, MM cells express a new FSTL5 transcript variant of unknown function. It would be of interest to investigate the function of this transcript variant and if it could have a role in the progression of MM.

Table of Contents

Abbreviations

AMH	Anti-Müllerian hormone
ASC	apoptosis-associated speck-like protein containing a caspase-activating recruitment domain
ASCT	autologous blood stem-cell transplantation
BMP	bone morphogenetic protein
BSA	bovine serum albumin
Caspases	cysteine-dependent aspartate-specific proteases
CRAB	hyper**c**alcemia, **r**enal failure, **a**nemia, and **b**one lesions
ESE	exonic splicing enhancers
ESS	exonic splicing silencers
ER	endoplasmic reticulum
FAM	6-carboxyfluorescein
FCS	fetal calf serum
FST	follistatin
FSTL1	follistatin-like 1
FSTL3	follistatin-like 3
FSTL4	follistatin-like 4
FSTL5	follistatin-like 5
GDF	growth and differentiation factor
GSP	gene specific primer
HCC	hepatocellular carcinoma
HMCLs	human myeloma cell lines
hnRNP	heterogeneous nuclear ribonucleoprotein

HRP	horseradish peroxidase
HS	human serum
ISE	intronic splicing enhancers
ISS	intronic splicing silencers
KD	knockdown
KO	knockout
LB	Luria Broth
MGUS	monoclonal gammopathy of uncertain significance
MM	multiple myeloma
mRNA	messenger RNA
ncRNA	non-coding RNA
PBS	phosphate-buffered saline
pre-mRNA	precursor mRNA
PTI	protein transport inhibitor cocktail
qRT-PCR	quantitative real-time PCR
RACE	rapid amplification of cDNA ends
RISC	RNA-induced silencing complex
RLU	relative light unit
RNA pol II	RNA polymerase II
RNA-seq	RNA sequencing
RT	reverse transcriptase
siRNA	small interfering RNA
SMM	smoldering multiple myeloma
SNP	single-nucleotide polymorphism
SR	serine- and arginine-rich

TAMRA	tetramethylrhodamine
TBS-T	Tris-buffered saline with Tween 20
TET	tetrachlorofluorescein
TGF-β	transforming growth factor-β
UP	universal primer
WT	wild type
3'UTR	three prime untranslated region

1. Introduction

1.1 Multiple myeloma and human myeloma cell lines

Multiple myeloma (MM) is a cancer characterized by the accumulation of antibody-producing plasma cells in bone marrow and their production of abnormal monoclonal immunoglobulin that are released into blood (1,2). MM is usually preceded by asymptomatic disorders including monoclonal gammopathy of uncertain significance (MGUS) and smoldering multiple myeloma (SMM) (3). Chromosomal rearrangement is commonly observed in MM patients. The translocation between an oncogene and an immunoglobulin gene could lead to the dysregulation of the oncogene that sometimes promotes the proliferation of plasma cells (4). As the subsequent genetic changes occur, the number of bone marrow plasma cells increases and the level of circulating monoclonal immunoglobulin rises and these changes gradually lead to "CRAB" symptoms (hyper**c**alcemia, **r**enal failure, **a**nemia, and **b**one lesions). Myeloma patients may also have neurological symptoms, infection, and amyloidosis. The explicit pathogenesis of MM is still unknown. However, there are several related risk factors, such as obesity, radiation exposure, and viral infection (5). Treatments for MM are applied only when patients develop symptoms (6). The fundamental strategy is to combine chemotherapy and autologous blood stem-cell transplantation (ASCT), however, it is restricted to patients with an age $\leq$ 65 years and without severe comorbidities (7). For patients over 65 years old or patients who could not tolerate ASCT, the therapy has been the combination of melphalan, prednisone, and thalidomide or bortezomib (6). Despite recent advances in improving treatment effects on MM patients, MM is still considered incurable regarding its high relapse rate in patients (8). Hence there is a need for developing novel therapies.

Human myeloma cell lines (HMCLs) are important tools to elucidate the pathogenesis of MM as well as to test novel therapies (9). The majority of HMCLs are derived from late-stage myeloma cells of different MM patients and vary in both phenotype and genotype (10). Although the relevance of HMCLs to MM has not been well-described *in vivo*, combining a set of heterogeneous HMCLs in *in vitro* experiments is still a good way to obtain relatively representative results and thus helps draw general conclusions for MM studies (10).

1.2 Transforming growth factor-β family

Transforming growth factor-β (TGF-β) family is a large group of secreted regulatory proteins that have similar structures (11). This family has over 30 members which are classified into several subgroups: TGF-βs, bone morphogenetic proteins (BMPs), activins and inhibins, growth and differentiation factors (GDFs), nodal, as well as Anti-Müllerian hormone (AMH) (11). The TGF-β family proteins play essential roles in regulating cell growth and migration and several proteins have been shown to be associated with MM (12). TGF-β triggers bone marrow stromal cells to secret IL-6, which is an important cytokine to promote the survival of MM cells *in vitro* (13). The BMPs inhibit the growth of myeloma cells and promote their apoptosis *in vitro* (14,15). Activin A had been found to induce osteolysis in MM and could also antagonize the growth-inhibiting effect of BMPs (16,17).

1.3 Follistatin and follistatin-like proteins

Follistatin (FST) was first discovered as a suppressive protein in regulating follicle-stimulating hormone secretion in ovarian follicular fluid (18). FST gene belongs to the follistatin family of genes and the FST protein is characterized by its three 10-cysteine structures which are termed as "follistatin domains" (18). Due to structural similarity, four other follistatin-like genes have been identified, which are follistatin-like 1 (FSTL1), follistatin-like 3 (FSTL3), follistatin-like 4 (FSTL4), and follistatin-like 5 (FSTL5). As demonstrated in Fig. 1, the Kazal-like domain, which is a highly conserved six-cysteine motif (19), is shared by all proteins of the follistatin family, whereas the follistatin-like domains are present in FST, FSTL1, and FSTL3. The EF-hand calcium-binding domains are shared by FSTL1, FSTL4, and FSTL5. FST and FSTL3 contain TGF-β binding domains, and FSTL4 and FSTL5 contain immunoglobulin-like domains. Except for these commonly shared domains, the von Willebrand factor C domain specifically presents in FSTL1 whereas the Asp/Glu-rich region is unique to FST. When comparing domain structures among the follistatin family of proteins, FST and FSTL3 are more structurally related to each other, and the same is the case for FSTL4 and FSTL5 (20).

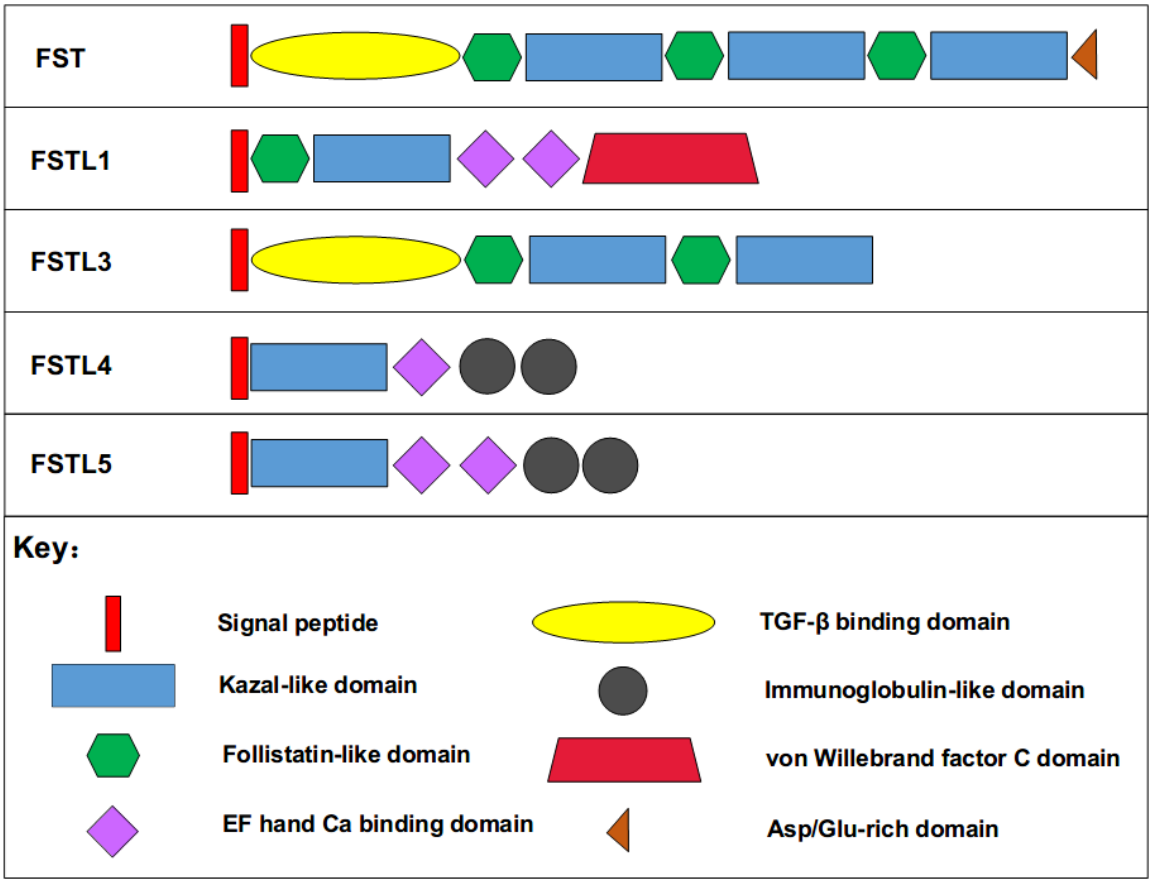

Figure 1. Domain structure of the follistatin family of proteins. Protein domains of FST, FSTL1, FSTL3, FSTL4, and FSTL5 are depicted. The signal peptide is presented at the N-terminus of each protein. The domains are arranged in the order of their locations on the amino acid chain.

FST and FSTL proteins are involved in regulating cell proliferation, differentiation and organogenesis, as well as tumor development (21–23). In addition, they act as antagonists in the TGF-β family. For instance, FST inhibits the activity of activin A and BMPs (24–26). FSTL1 was found to antagonize BMP-4 and also bind weakly to TGF-β1 (27). FSTL3 has been shown to bind activin A, myostatin, and some BMPs (28). Due to structural similarity, FSTL4 and FSTL5 are also hypothesized to be involved in regulating the signaling pathways of TGF-β family (18,29). However, neither of their functions have been well-characterized so far.

1.4 FSTL5

FSTL5 is a gene located on the q-arm of chromosome 4 in the human genome and consists of 16 exons that may give rise to several different splice variants (30). Five alternative transcripts (FSTL5-201, FSTL5-202, FSTL5-203, FSTL5-204, and FSTL5-205) with different lengths in base pairs have been described in the Ensembl database (31) so far: three of them encode proteins and two of them are processed transcripts which do not contain an open reading

frame. The transcript length in base pairs, the protein length in amino acids, as well as the predicted molecular weight of FSTL5 variants are described in Table 1. The protein-coding transcripts FSTL5-201 and FSTL5-202 contain all of the 16 exons, while FSTL5-203 lacks exon 11 (Fig. 2). In addition, FSTL5-203 does not contain a three prime untranslated region (3'UTR), which is presented in FSTL5-201 and FSTL5-202. The composition of the two non-coding transcripts is much more complicated due to splicing. FSTL5-204 includes part of sequences from intron 6, intron 8, and exon 9, as well as complete sequences from exon 7 and exon 8 (Fig. 2). FSTL5-205 contains part of sequences from exon 12 and intron 12 (Fig. 2). FSTL5 is expressed in certain types of human tissues and its RNA is especially enriched in brain and endocrine tissues (32). FSTL5 can also be detected with high gene expression levels in some cancer cell lines, such as Karpas 707, U-2197, HL-60, and U-266/70.

Table 1. Fundamental features of FSTL5 transcript variants. The information was retrieved from the Ensembl database (31).

Name of transcripts	Number of exons	Length of transcripts (bp)	Biotype	Number of amino acids	Molecular weight (kDa)
FSTL5-201	16	4796	Protein-coding	847	95.8
FSTL5-202	16	4793	Protein-coding	846	95.6
FSTL5-203	15	2920	Protein-coding	837	94.6
FSTL5-204	5	558	Processed transcript	No protein	—
FSTL5-205	2	404	Processed transcript	No protein	—

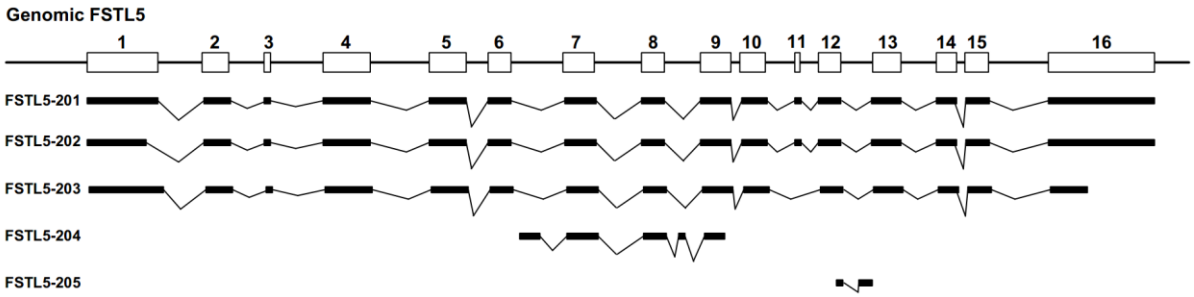

Figure 2. Schematic representation of FSTL5 transcript variants. White boxes represent exons that are numbered, and straight lines represent introns. Black squares underneath white boxes represent the partial or full length of exons or introns. The composition of each FSTL5 transcript variant is demonstrated by the black squares connected with broken lines.

The translation product of FSTL5 is predicted to be a secretory glycoprotein (33). All three FSTL5 protein isoforms harbor the same signal peptide which can be cleaved between position 20 and 21 of the amino acid chain (Appendix 1). The function of FSTL5 is largely unknown. By searching for FSTL5 on Google Scholar (https://scholar.google.com/), only a few publications had described this gene. Summaries of this gene and its translated protein in both physiological processes and diseases are mentioned below. Restricted expression of FSTL5 in the olfactory system of adult mouse brain implicated the potential role of FSTL5 in odor perception (33). By affinity capture-mass spectrometry, FSTL5 was shown to interact with the apoptosis-associated speck-like protein containing a caspase-activating recruitment domain (ASC) in cell-free extracts from THP-1 monocytes (34). Coding single-nucleotide polymorphisms (SNPs) in FSTL5 were related to thiopurine-associated bone marrow suppression in patients with inflammatory bowel disease (35). FSTL5 immunopositivity demonstrated prognostic value in different subtypes of medulloblastoma (36). In hepatocellular carcinoma (HCC), FSTL5 inhibited tumor cell growth, survival, and invasion by affecting Wnt/β-catenin signaling pathway (37,38). Down-regulated FSTL5 was associated with epithelial to mesenchymal transition process in HCC, which made it a promising target for treatment (39). Moreover, it was also proposed that FSTL5 could induce caspase-dependent apoptosis in HCC cells both in vitro and in vivo (40). In non-small cell lung cancer, mutations in FSTL5 in KRAS mutant cell lines were found to induce resistance to inhibitors of the nuclear export protein XPO1 (41). Interestingly, a recent paper compared the gene expression levels of different antagonists among normal plasma cells, MGUS cells, myeloma cells from patients, and HMCLs, and found that FSTL5 only had expression in the latter three groups of cells,

indicating its potential role in disease progression (42). In addition, FSTL5 was also found to be part of a high-risk signature in a subgroup of myeloma patients (10).

1.5 Gene transcription and alternative splicing

Genetic information is transferred from DNA to RNA by transcription and this process is dependent on polymerases. The transcribed DNA sequences are divided into two types: those protein-coding segments are called messenger RNAs (mRNAs), whereas the others are said to be non-coding RNAs (ncRNAs).

The product synthesized from the transcription of protein-coding DNA is called precursor mRNA (pre-mRNA), and it undergoes post-transcriptional modifications to be converted into mature mRNA, which is able to be exported from the nucleus to the cytoplasm and translated into protein afterwards (43). Post-transcriptional modifications involved in mRNA maturation mainly consist of three processes: 5’ end capping, 3’ end cleavage and polyadenylation, as well as RNA splicing (44). RNA splicing includes two different types: constitutive splicing and alternative splicing. In constitutive splicing, all introns are spliced out of the pre-mRNA and the exons are joined altogether to produce mature mRNA (45). Whereas in alternative splicing, exons are alternatively retained or removed and they are combined in various ways to synthesize multiple mRNA transcripts, which generates diverse protein isoforms in different cells and tissues as a result (45).

There are five basic modes of alternative splicing (Fig. 3). The most universal mode in eukaryotes is cassette exons, in which an exon may be spliced out of the pre-mRNA or just kept (46). Mutually exclusive exons denote that one of the two exons is retained in the final mRNA product, but never both (45). Alternative 5’ donor site selection allows the competition of 5’ splice sites with the upstream exon and results in the change of the 3’ boundary of that exon (47). Alternative 3’ acceptor site selection allows the competition of 3’ splice sites with the downstream exon, resulting in the change of the 5’ boundary of that exon (47). The final mode is called intron retention, which keeps a partial or complete intron in the mature mRNA product (45).

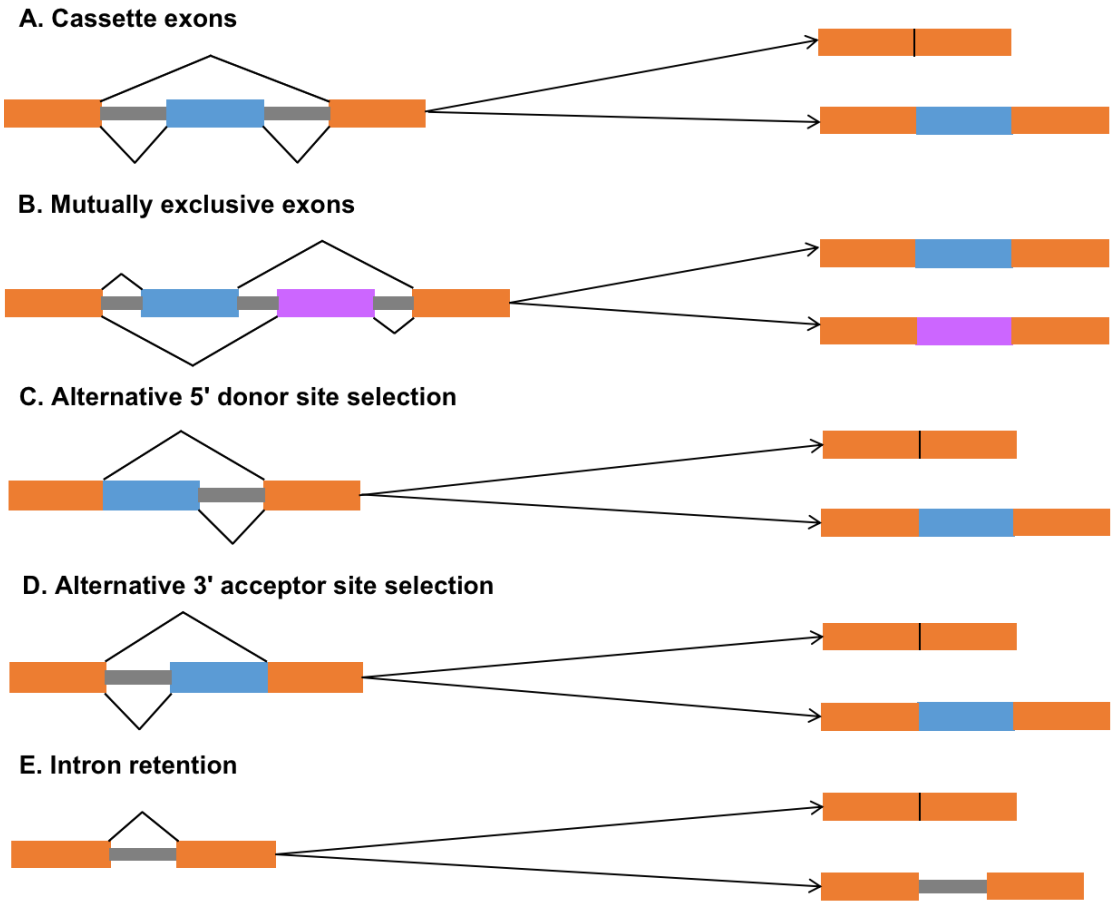

Figure 3. Different modes of alternative splicing. Five basic types of alternative splicing are depicted (A-E). The results of each type of splicing are shown on the right side of the figure, being pointed by arrows. Large boxes with orange, blue, and purple colors represent exons, and small gray boxes are introns. Cassette exons are the inclusion or exclusion of one or several independent exons (48). Mutually exclusive exons are the inclusion of one exon from an array of two adjacent exons. Alternative 5' or 3' splice site selection changes the boundary of exons and usually generates longer or shorter exons. Intron retention retains full or part of the intron in the mature transcript. The figure was adapted from (45) and recreated by BioRender (https://biorender.com/).

The regulation of alternative splicing is complex. Generally, it consists of two aspects: one is the interaction between trans-acting factors and cis-acting regulatory sequences and the other is the efficiency of RNA polymerase II (RNA pol II) (49). The trans-acting factor includes activators that promote splicing events and repressors that suppress splicing events (50). The majority of activators belong to the serine- and arginine-rich family of proteins (SR proteins) and most repressors are heterogeneous nuclear ribonucleoproteins (hnRNPs) (51,52). The SR proteins bind to their corresponding enhancer sequences such as exonic splicing enhancers (ESE) and intronic splicing enhancers (ISE), which promotes the assembly of the spliceosome and leads to exon splicing (51). In contrast, the hnRNPs recognize and bind to the silencer

elements such as exonic splicing silencers (ESS) and intronic splicing silencers (ISS), and thus inhibit the assembly of the spliceosome and result in the exclusion of exons (52). However, regulatory factors may sometimes demonstrate position-dependent properties in which the regulatory proteins might have opposite functions: for example, a splicing regulator promotes splicing when binding exonically to the upstream of the 5' splice site whereas suppresses splicing when binding intronically downstream of the 5' splice site (53,54). The efficiency of RNA pol II also affects splicing results (49). RNA pol II is a protein complex of the polymerase core with several subunits that works on transcribing DNA into pre-mRNA (55). Studies have found that high elongation rates of RNA pol II usually omits some weak splice sites during transcription and leads to exon skipping, while low elongation rates of RNA pol II can recognize the weak splice sites and results in normal splicing events (49). Apart from the predominant regulation aspects, alternative splicing can also be regulated at the epigenetic level through chromatin structure, histone modifications, DNA methylation, and even RNA modifications, making the regulation process more complicated (56).

By alternative splicing, one gene can encode several protein isoforms with varied or even conflicting functions, and therefore enrich the proteome from the restricted size of the genome (45). Alternative splicing has played significant roles in human body development as well as normal physiological processes (45). Some aberrant splicing events have been observed in many diseases, such as cystic fibrosis, growth hormone deficiency, and myotonic dystrophy (57,58). In addition, alternative splicing has also been involved in cancer. Altered expression of splicing factors, and mutations in splicing factors and regulators can lead to aberrant alternative splicing events, which may change the transcriptome of tumors (59). Some of these changes have been associated with the altered phenotypes of tumor cells, such as promoted cell proliferation and increased cell invasion ability (60,61). Based on this, it is possible to develop therapies targeted at splicing events to reverse abnormal phenotypes of cancer cells (60). Moreover, the aberrant alternative splicing events in cancer also provide information of prognosis in distinguishing cancer types and stages, which makes them potential tumor biomarkers (62).

1.6 Protein secretion process

Proteins that are secreted out of cells have an important role in intercellular communications for eukaryotes (63). Secretory proteins usually possess a signal peptide of 15-40 amino acids at the N-terminus (64). The sequences of the signal peptide are located in the

beginning part of an mRNA transcript that makes it firstly translated on the ribosome. The translated signal peptide is immediately recognized by signal-recognition particle, which halts the mRNA translation (65). The signal peptide - mRNA - ribosome complex is then directed to the endoplasmic reticulum (ER) and the halted translation restarts and produces the full-length amino acid chain which enters ER cavity afterwards. The signal peptide is removed by signal peptidases in ER and the left polypeptide chain undergoes modification, processing, and folding and is thereafter sent to Golgi for maturation (66). The mature proteins are secreted from Golgi to extracellular surroundings and execute their functions.

1.7 Caspases and their roles in apoptosis

Cysteine-dependent aspartate-specific proteases (Caspases) are a group of highly conserved proteases that specifically catalyze proteins containing aspartic acid residues by using their cysteine residue as the nucleophile during peptide bond cleavage (67). Caspases recognize and cleave protein substrates at specific peptide sequences, which mainly include the peptide sequence (W/L)EHD, the motif DEXD, and the sequence motif (I/V/L)E(H/T)D (68). Caspases play essential roles in the process of apoptosis and the involved candidates are caspase 3, 6, 7, 8, 9, and 10 (69). Caspases that trigger apoptosis are called initiators, including caspase 8, 9, and 10, and they are activated through dimerization after receiving upstream apoptotic signals (69). Activated initiator caspases then initiate the caspase cascade through catalyzing the cleavage of executioner caspases (caspase 3, 6, and 7) and these executioners directly degrade structural proteins and functional proteins in the cell, leading to apoptosis (69).

1.8 Aims

The specific aim of this thesis was to characterize the expression of both FSTL5 mRNA and protein in HMCLs. We also focused on testing and validating antibodies specific for FSTL5. In addition, we aimed to explore whether FSTL5, being a FSTL protein, could have an antagonizing effect of BMP and activins and to investigate what role it plays in cell survival. Finally, we expect to find out whether FSTL5 protein could be regulated by active caspases.

2. Methods

2.1 Myeloma cell lines and cell culture reagents

The HMCLs used in this project were IH-1, OH-2, KJON-1, VOLIN, URVIN, RPMI-8226, U-266, INA-6, ANBL-6, and JJN-3. All cell lines were cultivated at 37 °C in a humidified atmosphere containing 5% CO_2. The sources of these cell lines are different:

1) IH-1, OH-2, KJON-1, VOLIN, and URVIN were established in our laboratory (NTNU, Trondheim, Norway) (9,70,71);
2) RPMI-8226 and U-266 came from American Type Culture Collection (ATCC) (Rockville, MD, USA) (72,73);
3) INA-6 was a kind gift from Dr. Martin Gramatzki (University of Erlangen-Nurnberg, Erlangen, Germany) (74);
4) ANBL-6 was a kind gift from Dr. Diane F. Jelinek (Mayo Clinic, Rochester, MN, USA) (75);
5) JJN-3 was a kind gift from Dr. Jennifer Ball (University of Birmingham, Birmingham, UK) (76).

Cells were grown in RPMI-1640 medium (Sigma-Aldrich, St. Louis, MO, USA) mixed with L-glutamine (2 mM), hereafter called RPMI, and the supplementary serum added was either fetal calf serum (FCS) (Gibco, Thermo Fisher Scientific, Waltham, MA, USA) or human B+ serum (HS) (NTNU). In addition, IL-6 (Gibco) or IL-6 sup. (supernatant containing a mixture of cytokines including IL-6 from lipopolysaccharides-stimulated peripheral blood monocytes) was added depending on cell lines and growth and experimental conditions.

For the growth of IH-1, OH-2, and KJON-1, 10% HS (in volume) with IL-6 sup. was supplemented in the RPMI. The growth medium for INA-6 and ANBL-6 was supplemented with 10% FCS with 1 ng/mL IL-6. For VOLIN, JJN-3, U-266, and RPMI-8226, 10%, 10%, 15%, and 20% of FCS were added into the RPMI medium, respectively. URVIN was supplemented with 10% FCS with IL-6 sup. in the RPMI medium. The experiment medium was the same for all the cells, which contained 10% FCS and 1 ng/mL IL-6 in RPMI.

Moreover, INA-6 cells that were transfected with sgRNA-encoding lentivirus which targeted at FSTL5 exon 5 (CRISPR lentivirus, FSTL5, exon 5, HS0000117770) or FSTL5 exon

8 (CRISPR lentivirus, FSTL5, exon 8, HS0000117772) or non-targeting control (CRISPR-Lenti Non-Targeting Control Transduction Particles) were used in this thesis (all lentiviral particles were bought from Sigma-Aldrich), and they will be referred to as FSTL5 wild type (WT) and FSTL5 knockout (KO) in later sections. These cells were previously established and single-cell cloned in our laboratory. Western blots with antibody sc-246970 (also referred to as "antibody A" in the following contents) (Santa Cruz Biotechnology, Inc., Heidelberg, Germany) were used to pick clones that were potential FSTL5 KO cells. The growth condition for KO cells was the same as regular INA-6 cells, but the experimental conditions were different and would be illustrated in the specific experiment section. In this thesis, FSTL5 exon 5 KO, FSTL5 exon 8 KO, and FSTL5 WT clones were used.

2.2 Cell pellets, cDNA samples, drug, recombinant proteins, and inhibitors

Cell pellets from human embryonic kidney cells (HEK293), bone marrow stromal cells (Stroma), human liver cancer cells (HepG2), and mesenchymal stem cells (MSC) were already collected and provided by our laboratory. The cDNA samples from brain organoids AGC 1 and AGC 15 were kind gifts given by Dr. Wei Wang, NTNU. The drug, recombinant proteins, and inhibitory molecules used were as follows: BMP-6, activin B, and general caspase inhibitor Z-VAD-FMK were from R&D systems (Bio-Techne, Abingdon, UK); E. coli-produced and refolded activin A (human) was kindly provided by Marko Hyvönen's group at the University of Cambridge, UK (77); Myc-inhibitor (10058-F4) was bought from Sigma-Aldrich; Protein transport inhibitor cocktail (PTI) was from eBioscience Inc. (San Diego California, USA).

2.3 Quantitative real-time PCR

PCR is a method for amplifying specific DNA samples based on the mechanism of DNA replication. The whole reaction consists of 20-40 repeated cycles and each cycle contains three stages distinguished by discrete temperatures (78). The first stage is denaturation of the double-stranded DNA template by high temperature (95-100 °C), the next stage is annealing template-specific primers (50-65 °C), and the last stage is primer elongation by DNA polymerase (72 °C) (78). Quantitative real-time PCR (qRT-PCR), introducing fluorophores into PCR, serves as a quantitative method for detecting the initial amount of specific nucleic acid sequences by monitoring the change of fluorescence signal after each cycle. qRT-PCR is commonly used for studying mRNA expression. The mRNA needs to be reversely transcribed to cDNA by reverse transcriptase and the cDNA is amplified by PCR (79). The fluorochrome used in this project is a specific fluorescent reporter probe, which is also called the TaqMan probe. The sequences of

TaqMan probes are complementary to part of the cDNA templates (79). The probe is tagged with a fluorescent reporter at the 5' end and a quencher of fluorescence at the 3' end (Fig. 4A). The reporter fluorescence is quenched when probes are hybridized to cDNA strands. During the extension of PCR, probes are cleaved by Taq polymerase resulting in the release of the reporter and therefore allows the emission of fluorescent (Fig. 4B). The fluorescence signal against the number of cycles is displayed on an amplification curve (Fig. 5). During the exponential phase, there is a linear relationship between the quantity of DNA template and the logarithm of the amount of PCR product.

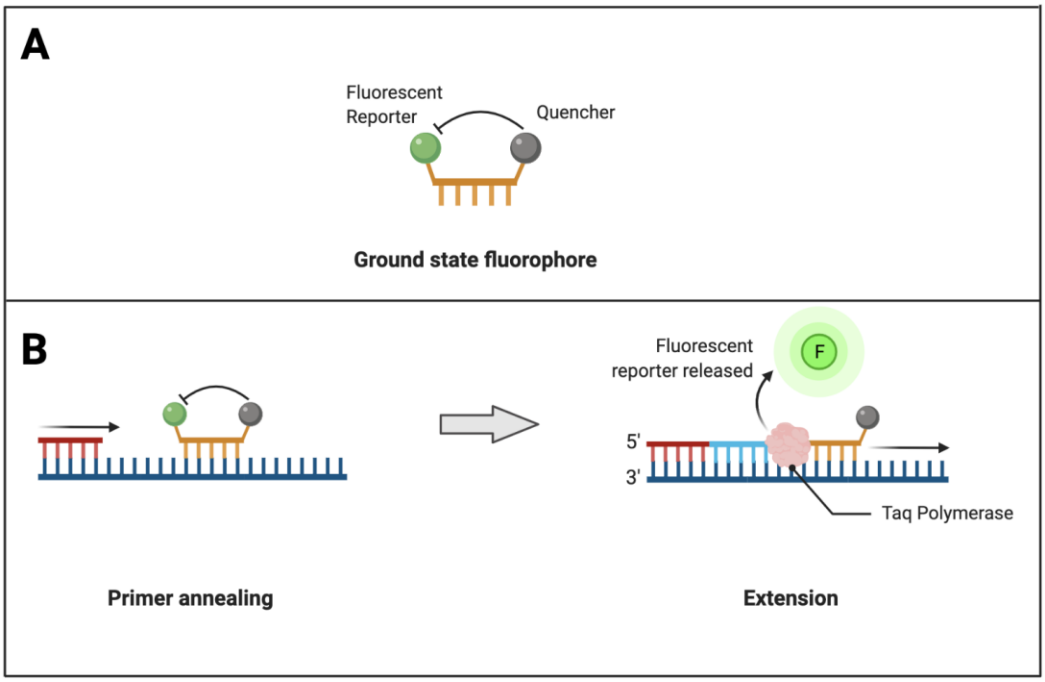

Figure 4. Fluorescence generation mechanism of the TaqMan probe. A) A TaqMan probe with a fluorophore in the ground state. The TaqMan probe is designed to be complementary to part of the target cDNA sequences to allow the annealing to the cDNA strand. The 5' end of the probe is attached by a fluorescent reporter and the 3' end is attached by a quencher molecule which inhibits the fluorescence signal from the reporter when they get close to each other. The fluorescent reporter can be either 6-carboxyfluorescein (FAM) or tetrachlorofluorescein (TET), and the quencher is usually tetramethylrhodamine (TAMRA) (80). B) The process of fluorescence production during qRT-PCR. The primer and probe first anneal to cDNA strands, followed by the extension of the nascent strand by Taq polymerase. During extension, the Taq polymerase degrades the probe and releases the fluorescent reporter, thereby generating a detectable fluorescence signal. Both figure A and B were created by BioRender (https://biorender.com/).

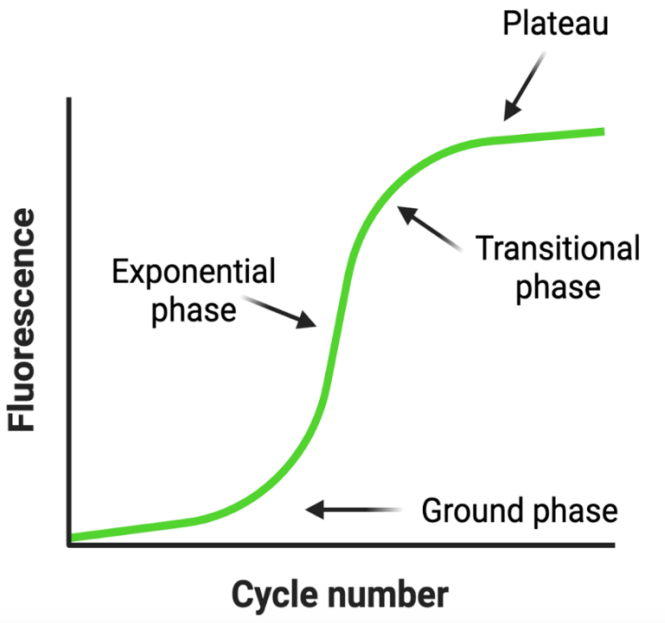

Figure 5. Amplification curve of qRT-PCR. The amplification curve is made with fluorescence as the y-axis and with cycle number as the x-axis. It represents the original results of qRT-PCR and consists of four phases: ground phase, exponential phase, transitional phase, and plateau. The figure was created by BioRender (https://biorender.com/).

Cells were centrifuged at 3400 rpm at 4 °C for 5 minutes and the precipitate was washed by phosphate-buffered saline (PBS) (R&D Systems) and centrifuged with the same settings again to harvest cell pellets which were then stored at -80 °C. Total RNA was extracted from cell pellets by using RNeasy Mini Kit (QIAGEN, Hilden, Germany) and its concentration was measured by NanoDrop™ 1000 Spectrophotometer (Thermo Fisher Scientific). Total RNA samples were made ready for the synthesis of cDNA using High-Capacity RNA-to-cDNA™ Kit (Applied Biosystems, CA, USA) and the whole reaction was run on C1000 Touch thermal cycler (Applied Biosystems) according to the program "HOTLID 105, 37 °C 60 min - 95 °C 5 min - 4 °C hold". The synthesized cDNA samples were diluted into 1 ng/µL and mixed with both PerfeCTa qPCR ToughMix (QuantaBio, MA, USA) and TaqMan Gene Expression Reagents (primers) (Applied Biosystems) (Table 2), and PCR was performed on StepOne™ Real-Time PCR System (Applied Biosystems). The comparative Ct method (ΔΔCt) was used for the analysis of relative expression of FSTL5 and the housekeeping gene GAPDH was chosen for normalization.

Table 2. TaqMan assays used for qRT-PCR.

TaqMan assay	Assay ID	Locations	Amplicon Length
GAPDH	Hs99999905_m1	GAPDH exon 2	122
FSTL5 primer pair 1	Hs01077017_m1	FSTL5 exon 3-4	88
FSTL5 primer pair 2	Hs00393783_m1	FSTL5 exon 6-7	87
FSTL5 primer pair 3	Hs01077014_m1	FSTL5 exon 15-16	151

qRT-PCR was performed in the following aspects: a) to explore FSTL5 mRNA expression in AGC 1, AGC 15, Stroma, MSC, HEK 293, HepG2, and INA-6 cells; b) to compare FSTL5 mRNA expression levels in HMCLs (URVIN, VOLIN, KJON-1, IH-1, OH-2, ANBL-6, INA-6, JJN-3, RPMI-8226, and U-266) and c) to evaluate FSTL5 mRNA expression in siControl and siFSTL5 INA-6 cells.

2.4 Rapid amplification of cDNA ends

Rapid amplification of cDNA ends (RACE) is a PCR-based method developed to generate the full-length sequence of cDNA ends from an interesting RNA transcript provided that a short internal sequence of this RNA is already known (81). The amplification of sequences can be between the small known internal sequence of the target mRNA and either its 5’ or 3’ end (5’-RACE or 3’-RACE) (81). Compared to traditional cDNA cloning methods, such as cDNA libraries screening, RACE is much cheaper and faster and needs only a small amount of RNA sample to generate considerably cDNA clones (81). There are some slight differences between 5’-RACE and 3’-RACE, however, the general process remains to be the same, which includes reverse transcription, PCR amplification, and product characterization. Here we only introduce 5’-RACE since it was performed to investigate the sequences of the 5’ end region of FSTL5 in INA-6 cells.

5’-RACE starts with first-strand cDNA synthesis primed by a modified oligo (dT) primer (Fig. 6). There are two important participants in the reverse transcription reaction: one is the SMARTScribe Reverse Transcriptase (RT) and the other is the SMARTer II A Oligonucleotide (82). The SMARTScribe RT adds 3-5 additional residues, primarily deoxycytidine, to the 3’ end of the first-strand cDNA by the action of its terminal transferase activity when it reaches the 5’ end of the mRNA template. The SMARTer II A Oligonucleotide then anneals to the

residues of the cDNA 3’ end and switches to a template for further cDNA strand extension by the SMARTScribe RT. The 5’-RACE-Ready cDNA serves as a template in RACE PCR and is amplified by forward universal primers (UPs) and reverse gene specific primer (GSP). In order to increase the amplification specificity, both long UP and short UP are introduced into the PCR reaction. The long UP and short UP share an inverted repeat element, whereas the long UP contains extra sequences complementary to the SMARTer II A Oligonucleotide. At the first round of PCR, the long UP anneals to the cDNA template and amplifies target sequences to avoid the production of unspecific cDNA products. The short UP and GSP then anneals to cDNA products from the first round to synthesis gene-specific fragments. The GSP contains a 15 bp extension which is homologous to the pRACE vector ends. The amplified 5’-RACE fragments are thereafter ligated into linearized pRACE vectors for sequencing.

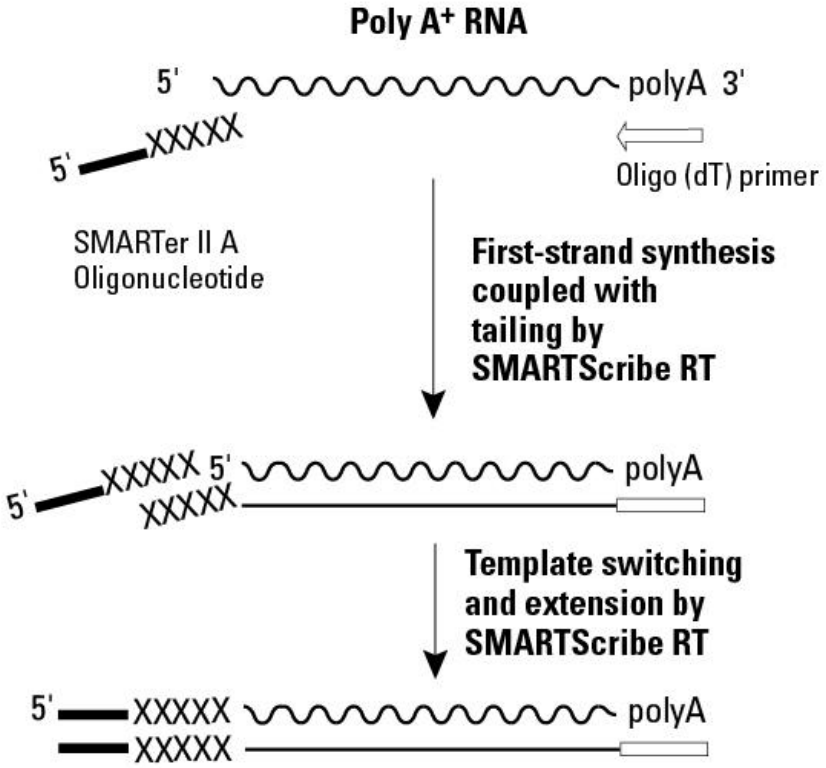

Figure 6. Mechanism of the 5’-RACE cDNA synthesis. The 5’-RACE cDNA synthesis starts with the annealing of Oligo (dT) primer and this reaction is catalyzed by SMARTScribe Reverse Transcriptase (RT). When the cDNA strand reaches the 5’ end of the template, the SMARTScribe RT adds a few non-templated residues that allow the annealing of the SMARTer II A Oligonucleotide to the cDNA strand. The SMARTer II A Oligonucleotide then switches to a template for the further cDNA strand extension by the SMARTScribe RT. The figure was from (82).

In this project, we have used the SMARTer® RACE 5'/3' Kit (TAKARA BIO Inc., Japan). Unless otherwise stated, all reagents mentioned in this section are included in this kit. Total RNA was extracted from INA-6 cells by RNeasy Mini Kit (QIAGEN). First-strand cDNA synthesis was performed in a 20 µL reaction system: 0.6 µg RNA sample mixed with 1.2 µM 5' CDS primer A, 2.4 µM SMARTer II A Oligonucleotide, 10 U SMARTScribe Reverse Transcriptase, 10 mM Dithiothreitol (DTT), 1X First-Strand Buffer, 2 mM dNTPs, as well as 1 U RNase Inhibitor. The sample mixtures were performed cDNA synthesis on C1000 Touch thermal cycler with settings of "42 °C 90 min, 70 °C 10 min". The 5'-RACE-Ready cDNA samples were then amplified in a 50 µL reaction system containing 200 nM GSP, 1X Universal Primer A Mix (UPM), 1.25 U SeqAmp DNA Polymerase, and 1X SeqAmp Buffer. In this project, we designed two GSPs for the FSTL5 gene, one towards exon 12 (FSTL5 short reverse primer) and the other towards exon 15 (FSTL5 long reverse primer) (exon numbering was based on the transcript variant FSTL5-203) (Table 3). 5'-RACE PCR was performed on the C1000 Touch thermal cycler (Applied Biosystems) with settings of 5 cycles of "94 °C 30 sec, 72 °C 3 min", 5 cycles of "94 °C 30 sec, 70 °C 30 sec, 72 °C 3 min", and 25 cycles of "94 °C 30 sec, 68 °C 30 sec, 72 °C 3 min". For PCR product characterization, 2 µL of the product was taken and analyzed on 2% agarose gels at 90 V for 45 minutes. After verification of the PCR product, the remaining 48 µL cDNA product was run on 2% agarose gels at 90 V for 45 minutes and the bands on the gels were excised and purified by using NucleoSpin Gel and PCR Clean-Up Kit (TAKARA BIO Inc.).

Prior to in-fusion cloning, the stellar competent cells (TAKARA BIO USA, Inc., CA, USA) were thawed on ice and mixed gently, and the in-fusion reaction mixture was made including the gel-purified RACE products and 1X In-Fusion HD Enzyme Premix as well as 50 ng linearized pRACE vector that contains M13 sequences. Thereafter, stellar competent cells were transformed with the in-fusion reaction mixture and incubated on ice for 30 minutes, followed by heat shock at 42 °C for 1 minute, and were incubated on ice again for 1 minute. The transformed cells were dissolved in 500 µL SOC medium (TAKARA BIO Inc.) and incubated on the shaker at 250 rpm at 37 °C for 1 hour. Each transformation was made into three tubes: 1/100 of the transformation (5 µL) was diluted in SOC medium to a total of 100 µL, 1/5 of the transformation (100 µL), and the rest of the transformation centrifuged to cell pellets and resuspended in 100 µL SOC medium. Each sample was spread on an individual Luria Broth (LB) plate with ampicillin and incubated in the incubator (Termaks, Bergen, Norway) at 37 °C overnight. The next day, plates growing with individually isolated colonies were selected and

three colonies from each plate were harvested. The picked colonies were grown in 2.5 mL LB medium with 50 µg/mL ampicillin in falcon tubes at 37 °C in a shaker (250 rpm) overnight. The plasmid DNA was isolated from the bacterial overnight culture by QIAprep Spin Miniprep Kit (QIAGEN). Isolated DNA samples were partially performed PCR by DreamTaq Hot Start PCR Master Mix kit (Thermo Scientific) using M13 primers (Integrated DNA Technologies, IA, USA) (Table 3) and the amplified samples were detected by 2% agarose gels at 90 V for 45 minutes to determine the positive RACE product inserts. The concentration of the plasmid DNA samples from miniprep was measured by Nanodrop and adjusted to 100 ng/µL by Milli-Q water. 5 µL of the 100 ng/µL plasmid DNA was mixed with 5 µL of 5 µM M13 forward or reverse primers and sent to the GATC Biotech company (Ebersberg, Germany) for sequencing. The sequencing results were analyzed on Benchling (https://www.benchling.com/).

Table 3. Primers used for 5'-RACE and sequencing. FSTL5 long reverse primer and FSTL5 short reverse primer are two GSPs that were involved in 5'-RACE PCR reaction. M13 forward and reverse primers are sequencing primers that were used both in selecting the RACE products that were inserted into vectors and sequencing the RACE products.

Primer	Sequence
FSTL5 long reverse primer	5' - GATTACGCCAAGCTTCAAACAAGCCACTGTCCTGGATTTGC - 3'
FSTL5 short reverse primer	5' - GATTACGCCAAGCTTCCCTCAGCTTTGGGACAGACTTCATC - 3'
M13 forward primer	5' - GTAAAACGACGGCCAGT - 3'
M13 reverse primer	5' - CAGGAAACAGCTATGAC - 3'

2.5 Western blot

Western blot is a commonly used technique in separating and identifying proteins of interest from cell lysates. The complete experiment consists of three procedures: protein separation, protein transfer, and protein detection (83). Proteins are first extracted from cells, followed by protein denaturation and gel electrophoresis separation. The sodium dodecyl sulfate polyacrylamide gel electrophoresis (SDS-PAGE) allows proteins to migrate from the negative pole to the positive pole (83). Proteins with different molecular masses have distinct migration speeds and move to different positions. The smaller the protein is, the faster it migrates in the gel. Proteins in the gel need to be transferred onto nitrocellulose membranes for detection. The protein transfer technique is called electroblotting, which uses an electric current to attract proteins with a negative charge moving from the cathode to the anode and the proteins are eventually immobilized to the nitrocellulose membrane. Prior to detecting the protein of interest, the membrane is incubated with a primary antibody which binds to the target protein specifically. The membrane is later exposed to a secondary antibody that recognizes the species portion of the primary antibody (83). The secondary antibody is labeled by a reporter, which can be either enzyme or fluorescent signal. In this project the horseradish peroxidase (HRP) substrate was used as the reporter, catalyzing chemiluminescent and generating a detectable luminescent signal (84) (Fig. 7).

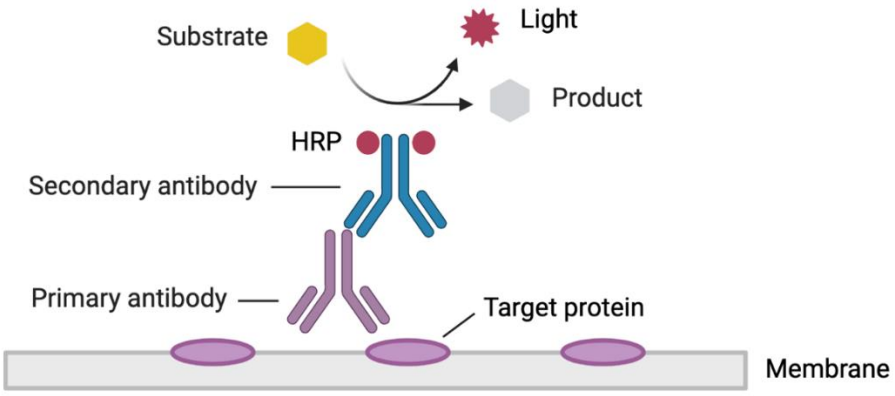

Figure 7. Protein detection by antibodies in western blot. The target protein on the nitrocellulose membrane can be recognized by the specific primary antibody, followed by the binding of an HRP-conjugated secondary antibody to the constant region of the primary antibody. The HRP can catalyze chemiluminescent substrates (usually luminol) and produce detectable light. The figure was adapted from (85) and recreated by BioRender (https://biorender.com/).

Cells were centrifuged at 1500 rpm, room temperature for 5 minutes and diluted to 1 million/mL in the experimental medium. One million of each sample were taken out and centrifuged at 3400 rpm at 4 °C for 5 minutes. Cell pellets were then washed by cold PBS and resuspended in a lysis buffer. The lysis buffer is composed of 1% of IGEPAL CA-630 (Sigma-Aldrich), 50 mM Tris, 150 mM NaCl, 10% glycerol, 1/10 tablet of cOmplete, Mini, EDTA-free Protease Inhibitor (Roche, Germany), 1 mM Na_3VO_4, and 1 mM NaF. Cell pellets dissolved in the lysis buffer were incubated on ice for 30 minutes, then centrifuged at full speed at 4 °C for 10 minutes and the supernatant (cell lysate) was transferred to new Eppendorf tubes. 15 µL of the cell lysate was mixed with 5 µL of SB/DTT (4X NuPAGE LDS Sample Buffer [Invitrogen, CA, USA] and 1 M Dithiothreitol) and heated at 70 °C for 10 minutes. SeeBlue™ Plus2 Pre-stained Protein Standard (Invitrogen) was applied as the ladder, and 20 µL of each sample mixture was loaded into each well of the gel. The gels used in this project were 4-12% NuPAGE Bis-Tris gels (Novex® by Life Technologies, CA, USA). Before gel electrophoresis, a running buffer was added into the buffer tank. Based on the differences in the sizes of the separated proteins, both 20X NuPAGE™ MOPS SDS Running Buffer (Invitrogen) and 20X NuPAGE™ MES SDS Running Buffer (Invitrogen) were used. Gel electrophoresis was then run under the condition of "80 V for 25 min, 150 V for 25 min, 180 V for 90 min". After gel running, the proteins on the gel were transferred onto nitrocellulose membrane under "20 V 1 min, 23 V 4 min, 25 V 2 min" by iBlot 2 Dry Blotting System (Invitrogen). The nitrocellulose membranes were first incubated with 5 % non-fat dry milk in 1X Tris-buffered saline with Tween 20 (TBS-

T) at a shaker at room temperature for 1 hour to block non-specific binding. Afterwards, they were incubated with primary antibodies at 4 °C for 1-3 days with shaking (Table 4A). Membranes were first washed by 1X TBS-T for 5 minutes three times and subsequently incubated with secondary antibodies at room temperature for 1 hour with shaking (Table 4B). Prior to detection, membranes were washed by 1X TBS-T for 10 minutes four times. In the end, they were incubated with HRP substrates Super-Signal West Femto (Thermo Fisher Scientific) for 4 minutes, and the pictures were captured by Odyssey Fc Imaging System (LI-COR Biosciences, Ltd., Cambridge, UK).

GAPDH was chosen as the protein control in this project. Membranes were incubated with primary Anti-GAPDH antibody (Table 4B) for 1 hour, and other steps were the same as the above paragraph.

Table 4. Antibodies used for western blot. A) Primary antibodies used for western blot. They were diluted in 2% non-fat dry milk in 1X TBS-T and stored at -20 °C. B) Secondary antibodies used for western blot. They were diluted in 1X TBS-T and stored at 4 °C.

A.

Catalog number	Referred in this thesis	Species/isoform	Immunogen	Dilution	Product source
sc-246970	**FSTL5 antibody A**	Goat polyclonal IgG	Peptide from an internal region of FSTL5 protein	1:500	Santa Cruz Biotechnology
ab105703	**FSTL5 antibody B**	Rabbit polyclonal IgG	Synthetic peptide from C-terminus of FSTL5 (amino acid 787-836)	1:500	Abcam, USA
ab167187	**FSTL5 antibody C**	Mouse polyclonal	Recombinant full-length FSTL5 protein (amino acid 1-847)	1:500	Abcam, USA
HPA045909	**FSTL5 antibody D**	Rabbit polyclonal IgG	Peptide from N-terminus of FSTL5	1:125	Sigma-Aldrich
NBP2-14028	**FSTL5 antibody E**	Rabbit polyclonal IgG	Peptide from central region of FSTL5	1:250	Novus, USA
H00056884-B01P	**FSTL5 antibody F**	Mouse polyclonal	Full-length FSTL5 protein	1:500	Abnova, Taiwan, China
9664	**Cleaved Caspase-3 (Asp175) (5A1E)**	Rabbit monoclonal	—	1:1000	CST, USA
ab8245	**Anti-GAPDH [6C5]**	Mouse monoclonal	—	1:30000	Abcam, USA

B.

Antibody name	Dilution	Product source
Polyclonal Rabbit Anti-Goat Immunoglobulins/HRP	1:2000	Dako Cytomation, Glostrup, Denmark
Polyclonal Goat Anti-Rabbit Immunoglobulins/HRP	1:3000	Dako Cytomation, Glostrup, Denmark
Polyclonal Goat Anti-Mouse Immunoglobulins/HRP	1:3000	Dako Cytomation, Glostrup, Denmark

Western blot was performed in the following aspects: a) to screen potential antibodies for detecting FSTL5; b) to compare protein levels displayed by different antibodies between HMCLs; c) to determine FSTL5-specific bands in FSTL5 KO cells and KD cells; d) to explore the effect of general caspase inhibitor on FSTL5 sizes in INA-6 cells.

2.6 siRNA transfection

Small interfering RNA (siRNA), usually 20 to 25 nucleotides in length, functions in one of the RNA silencing pathways to suppress the expression of specific genes (86,87). siRNA can be delivered into cells by transfection. When entering the cell, siRNA binds to the RNA-induced silencing complex (RISC) (88). One of the siRNA strands is selected as the guide strand and remains to bound to RISC while the other strand is degraded. The single-stranded siRNA directs RISC to combine with its target complementary mRNA sequences and as a result, a protein from RISC called argonaute catalyzes the cleavage of the mRNA, which prevents the target gene from being translated (88).

The siRNA transfection was performed as described before (89). In short, cells were diluted into 0.1 million/mL of the growth medium and incubated overnight. On the second day, cells were transferred into centrifuge tubes and spun down at 100 g for 10 minutes. After the removal of the supernatant, centrifuge tubes were put upside down to drain off excess liquids. Cell pellets were resuspended in transfection buffer R (100 µL/5 million cells/cuvette; Lonza, Basel, Switzerland) and transferred into cuvettes to mix with 2.5 µg vector pcDNA3-CD4 (a kind gift from Dr. M. Janz, Berlin, Germany) and 1 µM ON-TARGETplus Human FSTL5 siRNA - SMARTpool (Dharmacon, Lafayette, CO, USA) or 1 µM ON-TARGETplus Non-targeting Control siRNA (Dharmacon). Transfection was performed on Nucleofector^{TM} 2b

Device (Lonza) using program X-001 and after transfection, cells were immediately transferred to the pre-heated 10% FCS in RPMI with 1 ng/mL IL-6 at 0.5 million/mL and incubated overnight. The next day, CD4-expressing cells were selected by using Dynabeads™ CD4 Positive Isolation Kit (Invitrogen) and resuspended in 10% FCS in RPMI with 1ng/ mL IL-6. Cells transfected with siRNA were used in qRT-PCR, CellTiter-Glo, and western blot.

2.7 CellTiter-Glo® 2.0 Assay

CellTiter-Glo® 2.0 Assay (Promega, Madison, WI, USA) serves as a high sensitivity method for detecting cell viability through the presence of ATP produced by metabolically active cells (90). The reagent in this assay lyses the cells and the lytic cells release ATP which then participates in the luciferase reaction. The substrate luciferin in the assay can be catalyzed by the Ultra-Glo™ Recombinant Luciferase with the participation of ATP, molecular oxygen (O_2), and Mg^{2+}, and this reaction generates a luminescent signal that can be detected by a plate reader (Fig. 8). The measured light signal is in direct ratio to the ATP amount, which is in direct proportion to the number of viable cells (91).

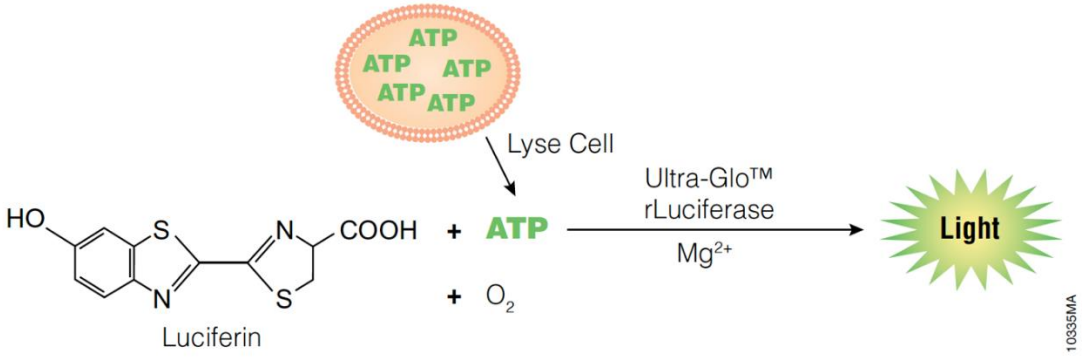

Figure 8. Mechanism of the CellTiter-Glo reaction. The luciferase catalyzes luciferin into detectable light in the presence of ATP, O_2, and Mg^{2+}. The ATP is produced by lysed cells. The Figure was from (90).

Cells were seeded in a 96-well opaque-walled plate with 10 000 cells per well and treated with different drug or recombinant proteins. The total volume for each well is 100 µL. After treatment, cells were incubated for 2 days in an incubator. Before reading luminescence, the 96-well plate was taken out from the incubator for heat dissipation at room temperature for 30 minutes and the CellTiter-Glo reagent was thawed in 22 °C water bath for preparation. 50 µL of the CellTiter-Glo substrate was added into each well by multichannel pipettes and the contents were mixed for 2 minutes on a shaker. After shaking, the mixture was incubated at

room temperature for 10 minutes and the plate was then put in the VICTOR Multilabel Plate Reader (PerkinElmer, Waltham, MA, USA) for luminescent signal detecting.

The CellTier-Glo assay was used to investigate the cell viability against different drug and recombinant proteins between FSTL5 WT and KO cells, and between siControl and siFSTL5 cells. The drug and recombinant proteins tested were 10058-F4 (20 µM and 40 µM), BMP-6 (5 ng/mL and 10 ng/mL), activin A (10 ng/mL and 20 ng/mL), and activin B (2.5 ng/mL and 5 ng/mL).

2.8 Statistics

The CellTiter-Glo results were analyzed by GraphPad Prism 9.0.0 (GraphPad Software, CA, USA) using the one-way ANOVA test. Results with a P value ≤ 0.05 were considered as statistically significant. The qRT-PCR data was analyzed by the ΔΔCt method with formula from (92) and the results were calculated by Microsoft Excel 2019.

3. Results

3.1 Expression of FSTL5 mRNA in different cell types and a panel of HMCLs

The expression of FSTL5 mRNA was previously investigated in a master thesis in our research group, but the primers used in qRT-PCR did not amplify any products. This was in contrast to the RNA sequencing (RNA-seq) data from Keats' lab which presented FSTL5 expression in a wide range of cell lines (93). In addition, several studies displayed FSTL5 mRNA expression in other cell types by PCR previously (33,38–40). We therefore wanted to explore more carefully FSTL5 mRNA expression in different cell types and a group of HMCLs.

We first analyzed FSTL5 gene expression in different cell types. We included cDNA from brain organoids (AGC 1 and AGC 15) as potential positive controls, since FSTL5 had been found to be highly expressed in brain tissue (32). The FSTL5 mRNA was reversely transcribed to cDNA and amplified by FSTL5 primers. Given that the transcripts expressed by these samples were unknown, three pairs of FSTL5 primers that were designed towards different exons were used (Table 2). All measured Ct values were presented in Table 5. As demonstrated by the Ct values, brain organoids AGC 1 and AGC 15 had got an expression of FSTL5 by using all three primer pairs and were therefore useful as positive controls for the FSTL5 primers. HEK293 and HepG2 had detectable mRNA levels, but the Ct values were very high, indicating that the expression was very low. INA-6 also had FSTL5 expressed at a similar level as brain organoid AGC 1, being detected by FSTL5 primer pair 3. This was in contrast to the previous master thesis that found no mRNA expression using primer pair 1 and primer pair 2 that span exons 3-4 and 6-7, respectively (94). No expression was shown in Stroma and MSC. The Ct values for GAPDH of these samples were between 21.8-22.8, indicating that the RNA isolation and cDNA synthesis was performed correctly.

Table 5. FSTL5 mRNA expression in different cell types and tissues. qRT-PCR was performed in brain organoids AGC 1 and AGC 15, Stroma, MSC, HEK293, HepG2, and INA-6. The primers used were towards different FSTL5 exons: FSTL5 primer pair 1 towards exon 3-4, FSTL5 primer pair 2 towards exon 6-7, and FSTL5 primer pair 3 towards exon 15-16. The expression of FSTL5 was described by the Ct values and the expression of housekeeping gene GAPDH implicated the good quality of the cell samples. The table represents the results of one experiment. The Ct Mean is the average Ct value of three parallel wells of each sample on the PCR plate and the Ct SD is the standard deviation of the three Ct values of one sample.

Tissue/cell line	GAPDH		FSTL5 primer pair 1 (exon 3-4)		FSTL5 primer pair 2 (exon 6-7)		FSTL5 primer pair 3 (exon 15-16)	
	Ct Mean	Ct SD	Ct Mean	Ct SD	Ct Mean	Ct SD	Ct Mean	Ct SD
AGC 1	22.8	0.3	27.1	0.3	28.2	0.1	31.4	0.1
AGC 15	22.7	0.6	31.6	0.3	33.5	0.3	36.7	0.2
Stroma	21.8	0.8	Not detectable		Not detectable		Not detectable	
MSC	22.2	0.3	Not detectable		Not detectable		Not detectable	
HEK293	22.8	0.3	Not detectable		Not detectable		35.7	0.6
HepG2	22.1	0.3	Not detectable		Not detectable		36	0.8
INA-6	22.8	1.2	Not detectable		Not detectable		31	0.2

According to the expression data, the FSTL5 primer pair 3 detected a PCR product in INA-6, which prompted us to apply this primer to investigate FSTL5 expression in other myeloma cells. We performed qRT-PCR in ten HMCLs (URVIN, VOLIN, KJON-1, IH-1, OH-2, ANBL-6, INA-6, JJN-3, RPMI-8226, and U-266) by using FSTL5 primer pair 3. The expression of FSTL5 was normalized by the expression of the housekeeping gene GAPDH in HMCLs, and the fold changes of each normalized cell line were calibrated using the cell line U-266, which represented 1-fold expression of FSTL5. Among these cell lines, VOLIN expressed the highest level of FSTL5 mRNA, followed by KJON-1, INA-6, U-266, IH-1, and URVIN (Fig. 9). However, RPMI-8226, JJN-3, OH-2, and ANBL-6 showed no expression. In conclusion, the FSTL5 mRNA showed expression in brain tissue as well as in several HMCLs.

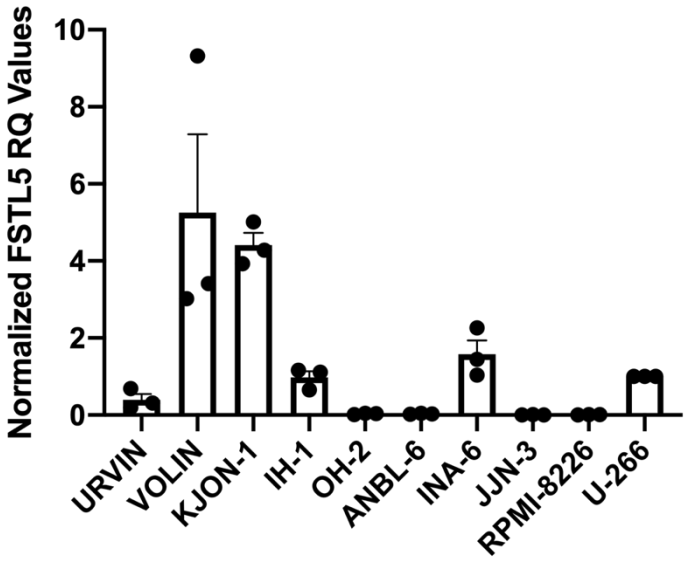

Figure 9. Comparison of FSTL5 mRNA levels across HMCLs. qRT-PCR was performed in URVIN, VOLIN, KJON-1, IH-1, OH-2, ANBL-6, INA-6, JJN-3, RPMI-8226, and U-266 by using FSTL5 primer pair 3. The relative expression of FSTL5 was described by the ΔΔCt method with GAPDH as a housekeeping gene. The figure represents the results of three repeats. Each dot represents the normalized expression level for one repeat (fold changes in each cell line were normalized to U-266), each bar represents the mean value of three repeats, and the error bars represent the standard error of the means.

3.2 Rapid amplification and sequencing of FSTL5 cDNA 5' ends in INA-6

Our mRNA expression data showed that in INA-6 cells, FSTL5 primer pair 1 (exon 3-4) and FSTL5 primer pair 2 (exon 6-7) failed to amplify FSTL5 cDNA, whereas the FSTL5 primer pair 3 (exon 15-16) did provide amplification products. In order to figure out why primers spanning the first few exons failed to amplify FSTL5, we performed 5'-RACE experiment to obtain the 5' ends of FSTL5 cDNA in INA-6 cells.

3.2.1 Amplification of FSTL5 cDNA 5' ends

The 5'-RACE PCR was performed to amplify the FSTL5 gene 5' end regions from INA-6 cells by the designed GSPs. The FSTL5 short reverse primer amplified a fragment between 650-850 bp, whereas the size of the FSTL5 long reverse primer product was between 1000-1500 bp (Fig. 10A).

3.2.2 Sequencing of FSTL5 cDNA 5' ends

Before sequencing, the RACE PCR products from both RACE primers were purified and cloned into pRACE plasmid. The purified products were named S1-S3 (products from FSTL5 short reverse primer) and L1-L3 (products from FSTL5 long reverse primer) for distinction. To

determine the positive inserts, all products were amplified by M13 forward and reverse primers and analyzed by gel electrophoresis. As shown in Fig. 10B, all RACE products were successfully inserted into pRACE vectors. Each RACE-plasmid product was sequenced by either M13 forward primer (F) or M13 reverse primer (R), and the "F" or "R" was added behind S1-S3 and L1-L3 to use as the name for sequencing products. The length of the sequencing products (S1R/F, S2R/F, S3R/F, L1R/F, L2R/F, L3R/F) was 1217 bp, 1235 bp, 1143 bp, 1229 bp, 1206 bp, 1225 bp, 685 bp, 1165 bp, 728 bp, 1163 bp, 771 bp, and 1189 bp, respectively. All product sequences were aligned with FSTL5-203 as a template (Fig. 10C, Appendix 2). The gray areas represent sequences that were the same as the template while the red areas represent mismatches. The regions of sequences marked by blue boxes were originated from the pRACE vector. The regions marked by yellow boxes were sequences of the SMARTer II A Oligonucleotide. The sequences in green boxes shared by all products did not align with either pRACE vector or SMARTer II A Oligonucleotide, and by blasting them we found that they were partial sequences of FSTL5 intron 6. The RACE products S1-S3 started from FSTL5 exon 7 and ended at the position where the FSTL5 short reverse primer annealed (FSTL5-203, exon 12). In addition, deletion of FSTL5 exon 8 and a point mutation (G>A) at position 1487 was detected in product S1 and S3, respectively. The products L1-L3 started from FSTL5 exon 7 and ended at the position where the FSTL5 long reverse primer annealed (FSTL5-203, exon 15). Besides, in L1, we identified one point mutation (C>T) at nucleotide position 1671. In L3, two point mutations and two indels were detected: position 1883 C>T, position 2080 A>T, position 2079 delA, and position 2259 insA. Based on the data from the RACE analysis, it seemed like the FSTL5 transcript in INA-6 started at intron 6 and ended at least exon 15 where the FSTL5 long reverse primer annealed, and the first transcribed exon was number 7 (Fig. 10D).

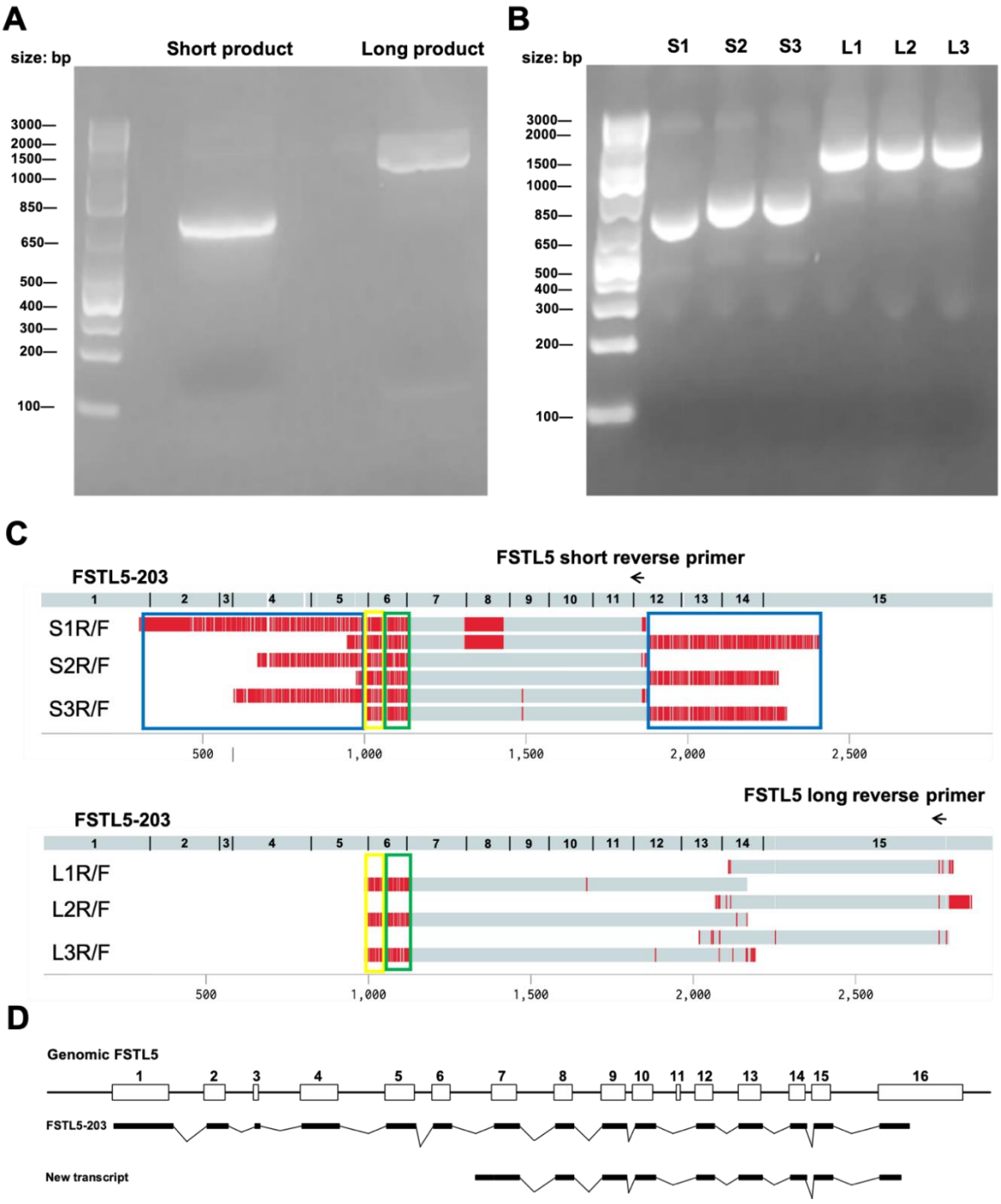

Figure 10. Rapid amplification and sequencing of FSTL5 cDNA 5' ends in INA-6. Total RNA from INA-6 cells was reversely transcribed into cDNA, amplified by GSPs, infusion-cloned into pRACE vectors, miniprepped, and sequenced. A) cDNA from reverse transcription was amplified in PCR by FSTL5 short reverse primer and long reverse primer and the products were separated by 2% agarose gel. B) The separated PCR products on the gel were purified and in-fusion cloned into pRACE plasmid and miniprepped and then separated by 2% agarose gel (S1-S3: products from FSTL5 short reverse primer; L1-L3: products from FSTL5 long reverse primer). C) The miniprepped products were sequenced and the sequencing results of short and long primer products were aligned with FSTL5-203 ("R" and "F"

represent M13 reverse primer and M13 forward primer, respectively). Primer positions were displayed by the arrows. Blue boxes represent the sequences of pRACE vector. Yellow boxes represent the sequences of SMARTer II A Oligonucleotide. Green boxes represent the sequences of FSTL5 intron 6. D) Schematic representation of the new FSTL5 transcript.

3.3 Comparison of FSTL5 antibodies and expression of their corresponding proteins in HMCLs

Both FSTL5 expression patterns in myeloma cells and FSTL5 antibodies' performances are undetermined. The earlier results obtained in the lab by F. Alemu Atire and others were done with one antibody, FSTL5 antibody A (94). This antibody had detected bands at approximately 97 kDa, which fit with the predicted full-size of FSTL5 protein. However, from both qRT-PCR and 5'-RACE results, it was a great possibility that FSTL5 is only expressed as part of its full-length transcript in HMCLs, so the previous bands detected with antibody A might not represent the actual FSTL5 protein form in HMCLs. We therefore decided to compare a few commercially available antibodies to get a clearer impression on the potential protein expression in HMCLs. Six FSTL5 antibodies (named A-F for convenience, Table 4) recognizing various parts of FSTL5 protein had been tested to compare different antibodies' detection abilities (Appendix 3). The results showed that antibody A, B, D, and E displayed clear bands at specific positions (97 kDa, 97 kDa, 97 kDa, and 64 kDa, respectively) that varied between different cell culture conditions. Since the expression patterns of FSTL5 displayed by antibody B and D were similar and antibody B showed stronger bands, we decided to include antibody B in the following experiments. Based on the above, we finally selected antibody A, B, and E to test FSTL5 protein as well as to compare their performances.

FSTL5 is predicted as a secretory glycoprotein based on the presence of a signal peptide (Appendix 1). PTI is a cocktail of Brefeldin A and Monensin, which prevents the secretory proteins from being transported to the extracellular space (95). Treating cells with PTI leads to the accumulation of secretory proteins in ER and Golgi, which can be detected by western blot after cell lysis. To further validate whether FSTL5 could be secreted and to compare FSTL5 protein levels in different HMCLs, we performed western blot with cells treated with/without PTI, and the results were shown in Fig. 11.

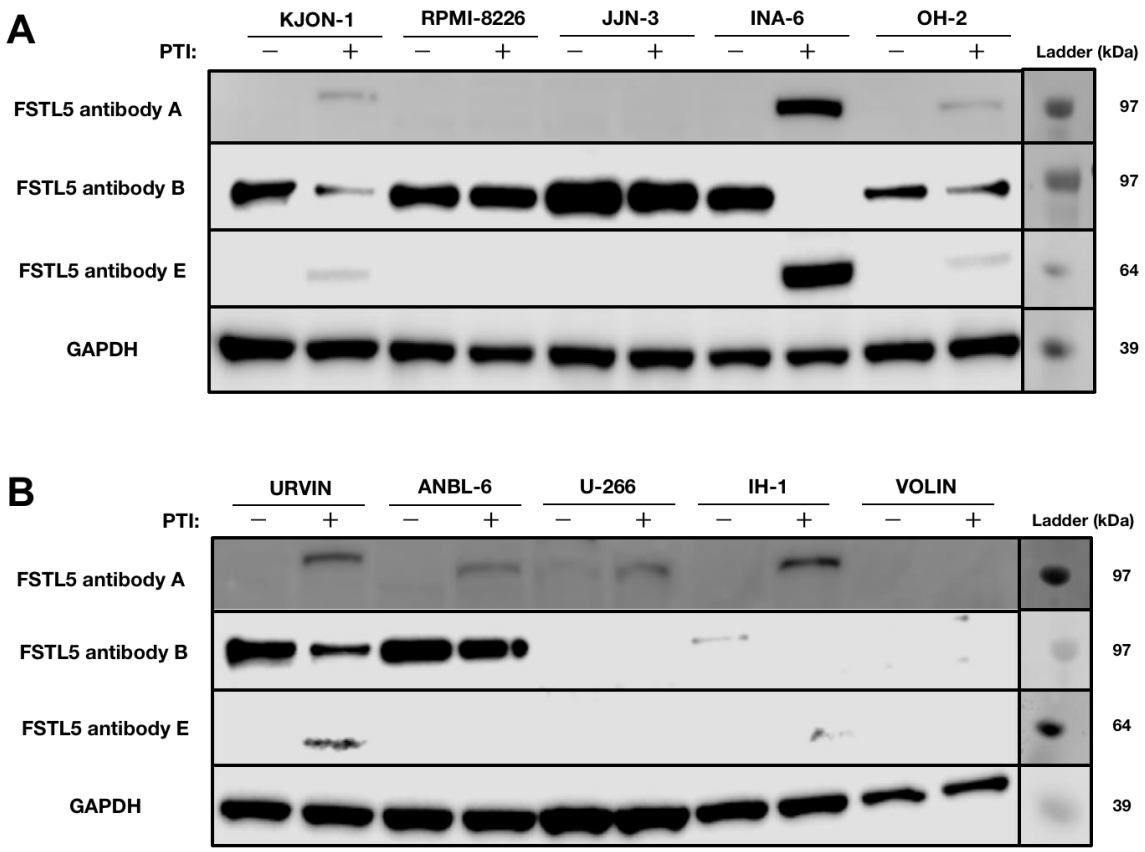

Figure 11. Comparison of FSTL5 protein levels in HMCLs. Cell lines displayed in Fig. A (KJON-1, RPMI-8226, JJN-3, INA-6, and OH-2) and Fig. B (URVIN, ANBL-6, U-266, IH-1, and VOLIN) were incubated in 10% FCS (in RPMI with 1 ng/mL IL-6) with or without PTI for 4 hours. The cells were then used for western blot with FSTL5-targeting antibody A, B, and E. GAPDH antibody was used as the loading control. The figure shows one representative result of three repeats.

A 97 kDa protein, which fit with the predicted full-size FSTL5, was detected with antibody A in KJON-1, INA-6, OH-2, URVIN, ANBL-6, U-266, and IH-1, all being treated with PTI. Among these cell lines, INA-6 showed the highest protein levels, followed by IH-1 and URVIN. The protein amount in KJON-1, OH-2, ANBL-6, and U-266 showed no significant difference, and all were less than URVIN. No protein was seen in RPMI-8226, JJN-3, and VOLIN.

A protein of 97 kDa was detected with antibody B in KJON-1, RPMI-8226, JJN-3, INA-6, OH-2, URVIN, ANBL-6, and IH-1. This also fit with the full-length FSTL5. In KJON-1, RPMI-8226, JJN-3, OH-2, URVIN, and ANBL-6, it was seen in both PTI-treated and non-treated cells, whereas the protein levels in PTI-treated cells were decreased compared to non-PTI treatment. In INA-6 and IH-1, the 97 kDa protein was only shown in non-PTI-treated cells. No protein was detected in U-266 and VOLIN.

Antibody E displayed a 64 kDa protein in KJON-1, INA-6, OH-2, and URVIN, all being treated with PTI. INA-6 presented the highest level of it among these cells, followed by URVIN. The 64 kDa protein amount in KJON-1 and OH-2 showed no significant difference, and both were less than URVIN. No protein was detected in RPMI-8226, JJN-3, ANBL-6, U-266, IH-1, and VOLIN. To sum up, three FSTL5 antibodies displayed different protein expression patterns in HMCLs and it was hard to determine the correct form of FSTL5 from this result.

3.4 Genetic knockout and knockdown of FSTL5 in INA-6

Based on previous results from western blot, it's crucial to confirm that FSTL5 antibodies recognize and bind to their targets in the right way. Appropriate negative controls are essential in validating antibodies' specificity and are also good ways to explore the functions of the gene. There are two common methods used as negative controls, one is gene knockout (KO) and the other is gene knockdown (KD).

3.4.1 FSTL5 KO in INA-6 cells

3.4.1.1 Antibody validation in KO cells

CRISPR/CRISPR-associated protein 9 (CRISPR/Cas9) is a frequently adopted initiative of gene KO. Through CRISPR/Cas9 technique, the expression of the targeted protein would be suppressed which could not be detected by specific antibodies. Earlier, an attempt had been made in the laboratory to make FSTL5 KO INA-6 cells (94). The possible FSTL5 KO clones had been picked based on the protein bands detected with antibody A and we were therefore not sure if they were real KO cells. We still decided to test them to see if it was possible to reproduce the earlier results and if changes in protein levels could be detected with any of the other antibodies. Hence in this experiment, FSTL5 WT and KO INA-6 cells were incubated in 10% HS or 0.1% bovine serum albumin (BSA) (Gibco) with/without PTI and the protein levels were analyzed by antibody A, B, and E. Compared to 10% HS that is suitable for INA-6 growth, 0.1% BSA contains fewer cell growth factors that provides a poor culture condition for cells and promotes cell apoptosis (94). Different experimental conditions might affect the expression of FSTL5 protein. The experiment was performed twice, but the results had poor reproducibility. Here we selected one of the results and displayed it in Fig. 12, and the other could be seen in Appendix 4.

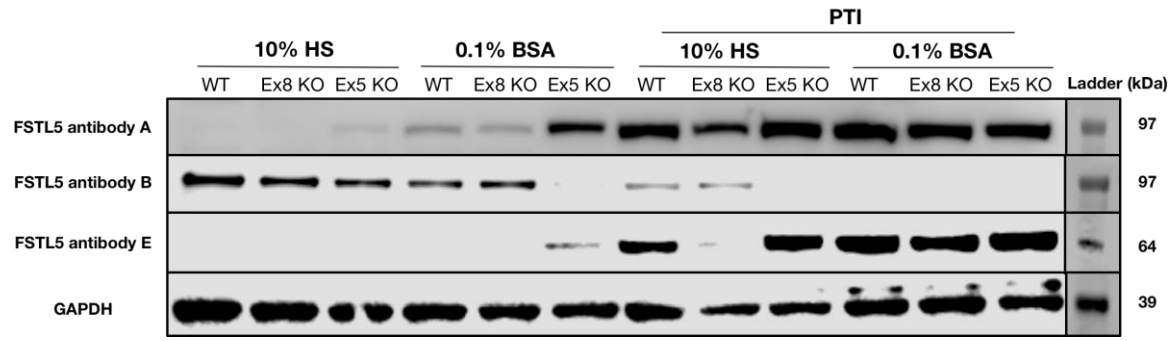

Figure 12. Validation of antibodies with FSTL5 KO cells. FSTL5 KO cells (FSTL5 exon 5 KO and FSTL5 exon 8 KO) and FSTL5 WT control cells were incubated in 10% HS (in RPMI with 1 ng/mL IL-6) or 0.1% BSA (in RPMI) with/without PTI for 4 hours. The cells were then used for western blot with FSTL5 antibody A, B, and E. GAPDH antibody was used as the loading control. The figure shows one of the two irreproducible results.

For antibody A, the 97 kDa protein levels were higher in the presence of PTI, or in 0.1% BSA. In 10% HS treated group, the protein was detected in FSTL5 exon 5 KO cells with a weak signal and it was not shown in control and exon 8 KO cells. In 0.1% BSA treated group, the 97 kDa protein was expressed by all cell lines. Compared to control, the protein in exon 8 KO cells was slightly decreased whereas it was apparently increased in exon 5 KO cells. In 10% HS and PTI treated group, the protein was obviously decreased in exon 8 KO cells and was slightly increased in exon 5 KO cells compared to the control. In 0.1% BSA and PTI treated group, protein levels displayed no significant difference between exon 5 and exon 8 KO cells, and all were mildly reduced compared to WT cells.

The 97 kDa protein detected with antibody B showed lower levels in the presence of PTI, or in 0.1% BSA. In 10% HS treated group, the protein was detected in WT, exon 8 KO, and exon 5 KO cells, and the amount was reduced sequentially. In 0.1% BSA treated group, the protein was only detected in WT and exon 8 KO cells and the amount was similar between them. In 10% HS and PTI treated group, the 97 kDa protein was shown in WT and exon 8 KO cells with an even amount. No protein was seen in 0.1% BSA and PTI treated group.

The 64 kDa protein displayed by antibody E showed higher levels in the presence of PTI, or in 0.1% BSA. In 10% HS treated group, the protein was not detected in any cell line. In 0.1% BSA treated group, it was only shown in exon 5 KO cells. In 10% HS and PTI treated group, the protein in exon 8 KO cells was clearly decreased whereas its levels showed a slight increase in exon 5 KO cells compared to the control. In 0.1% BSA and PTI treated group, the protein in exon 8 KO cells was slightly reduced compared to the control and exon 5 KO cells. In summary,

the proteins detected with antibody A and antibody E showed a decrease in FSTL5 exon 8 KO cells and the protein detected with antibody B showed a decrease in FSTL5 exon 5 KO cells.

3.4.1.2 Different drug's and recombinant proteins' effect on FSTL5 WT and FSTL5 KO cells

The RACE data displayed that the FSTL5 expressed by INA-6 began with exon 7, which indicated that the KO of exon 5 might not suppress the protein expression in INA-6. Combining with the western blot results, we speculated that the FSTL5 exon 8 KO cell line, rather than FSTL5 exon 5 KO cell line, might be a potential KO cell line and we therefore used FSTL5 exon 8 KO cell line in this section. To check if the potential KO of FSTL5 would affect the effect of possible inhibitory molecules and TGF-β family proteins, one drug and three recombinant proteins (10058-F4, BMP-6, activin A, and activin B) were tested using FSTL5 WT and FSTL5 KO cells. 10058-F4 is a Myc inhibitor that promotes cell-cycle arrest and leads to apoptosis. BMP-6, activin A, and activin B are recombinant proteins of the TGF-β family. The results showed that there was no significant difference between them in the sensitivity towards any of the factors (Fig. 13).

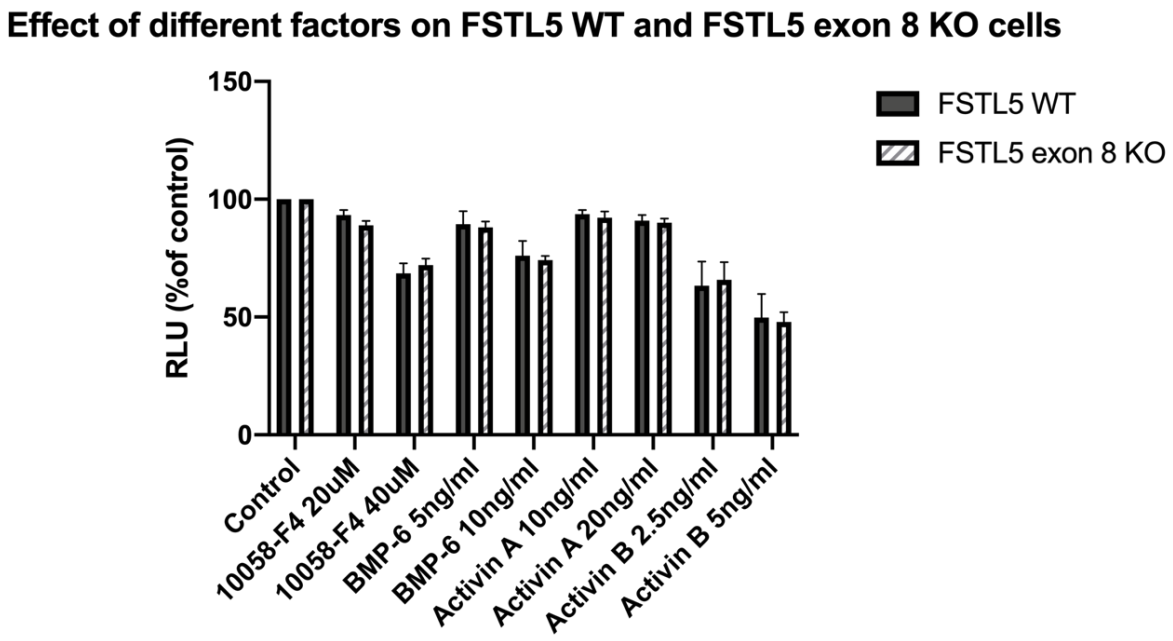

Figure 13. Comparison of different factors' effect between FSTL5 WT and FSTL5 exon 8 KO cells. One drug and three recombinant proteins with different doses were used: 10058-F4 20 μM and 40 μM; BMP-6 5 ng/mL and 10 ng/mL; activin A 10 ng/mL and 20 ng/mL; activin B 2.5 ng/mL and 5 ng/mL. The figure represents the average results of three repeats. The relative light unit (RLU) for each treatment was normalized to that of the nontreatment control. Each bar represents the mean value of RLU from three repeats and each error bar represents the standard error of the mean. Results with a P value ≤ 0.05 were considered as significant.

3.4.2 FSTL5 KD in INA-6 cells

3.4.2.1 Antibody validation in KD cells

The puzzling results from CRISPR KO cell lines prompted us to add an alternative verification strategy, gene KD, in this project. KD by small RNA interference was applied in this project. To suppress FSTL5 mRNA and hopefully thereby protein expression, siRNAs were inserted into INA-6 cells by transfection. We first checked FSTL5 mRNA expression level by qRT-PCR. Compared to non-targeting control siRNA, FSTL5 siRNA decreased FSTL5 levels by 50% (Fig. 14A), which provided a good indication for the success of FSTL5 gene KD in INA-6 cells. We then treated siRNA-induced cells with/without PTI and performed western blot on these cells. The results were shown in Fig. 14B, antibody A and E respectively displayed clear bands at 97 kDa and 64 kDa that showed strong signals in both PTI treated siControl and siFSTL5 cells, and slightly decreased protein levels were detected in siFSTL5 cells. The 97 kDa protein detected with antibody B was shown in non-PTI-treated siControl and siFSTL5

cells, and compared to siControl, the protein amount even increased in siFSTL5 cells. Concisely, the proteins detected with antibody A and antibody E were decreased in FSTL5 KD cells whereas the protein detected with antibody B was even increased in FSTL5 KD cells.

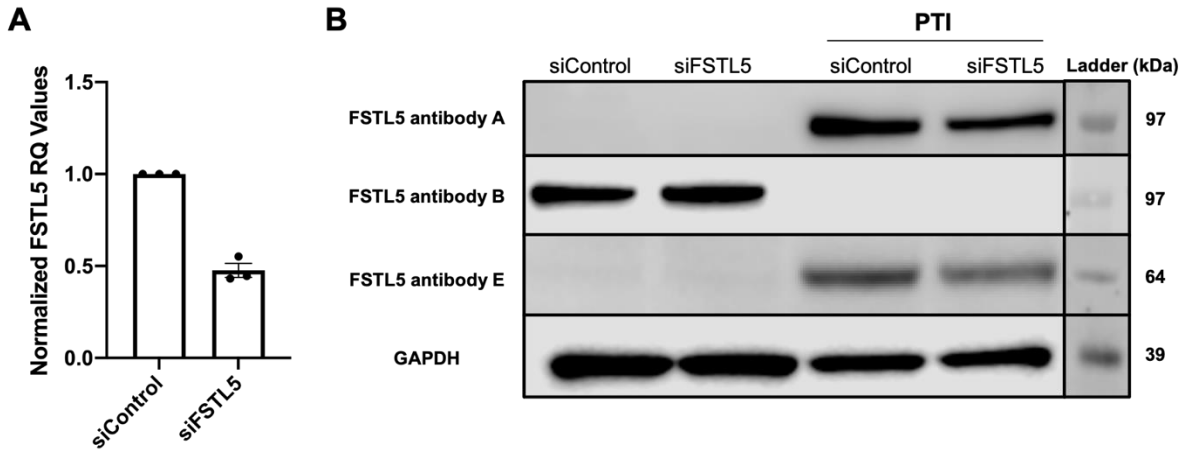

Figure 14. Validation of antibodies with FSTL5 KD cells. INA-6 cells were transfected with non-targeting control siRNA and FSTL5 siRNA. A) qRT-PCR was performed to examine the FSTL5 mRNA levels between siControl and siFSTL5 cells. Fig. A represents the average results of three repeats. Each dot represents normalized Ct value for one repeat (fold changes in siFSTL5 were normalized to siControl), each bar represents the mean Ct value of three repeats, and each error bar represents the standard error of the mean. Results with a P value ≤ 0.05 were considered as significant. B) siControl and siFSTL5 cells were treated in 10% FCS (in RPMI with 1 ng/mL IL-6) with and without PTI for 4 hours. Western blot was performed after treatment by using antibody A, B, and E. GAPDH antibody was used as the loading control. Fig. B displays one representative result of three repeats.

3.4.2.2 Different drug's and recombinant proteins' effect on siControl and siFSTL5 cells

To check if the knockdown of FSTL5 would influence the effect of possible inhibitory molecules and TGF-β family proteins, the same drug and recombinant proteins as that were applied in FSTL5 KO cells were tested using siControl and siFSTL5 cells. Compared to siControl cells, which were considered the same as the normal INA-6 cells, siFSTL5 cells showed no potentiation in the sensitivity towards any of the drug or recombinant proteins (Fig. 15).

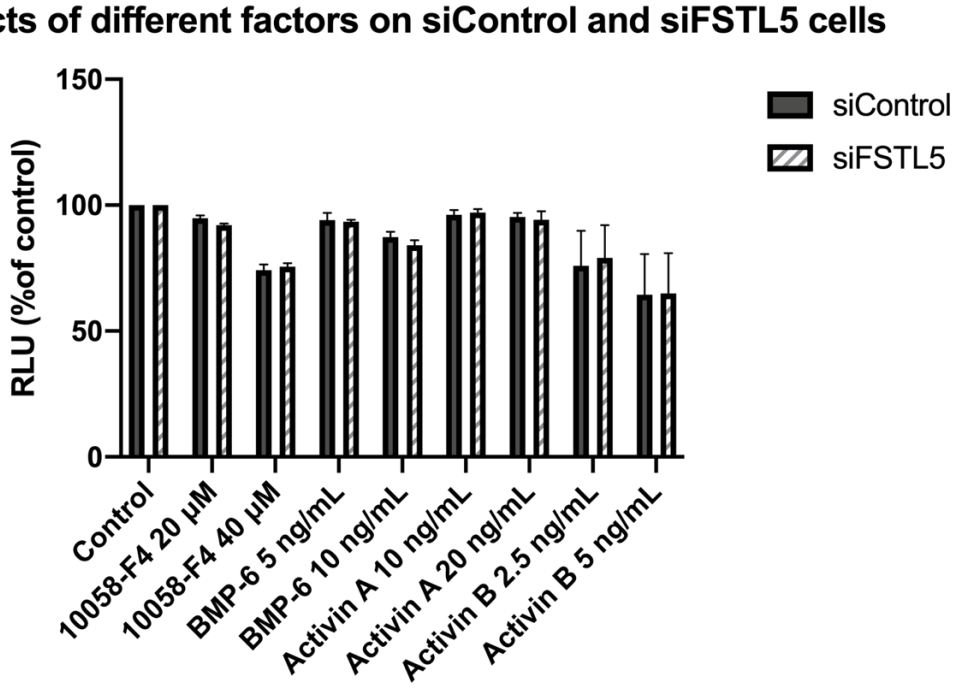

Figure 15. Comparison of different factors' effect between siControl and siFSTL5 cells. One drug and three recombinant proteins with different doses were used: 10058-F4 20 μM and 40 μM; BMP-6 5 ng/mL and 10 ng/mL; activin A 10 ng/mL and 20 ng/mL; activin B 2.5 ng/mL and 5 ng/mL. The figure represents the average results of three repeats. The RLU for each treatment was normalized to that of the non-treatment control. Each bar represents the mean value of RLU from three repeats and each error bar represents the standard error of the mean. Results with a P value ≤ 0.05 were considered as significant.

3.5 Influence of general caspase inhibitor on the potential FSTL5 protein sizes in INA-6

A former master thesis had found that the caspase inhibitors could have an impact on the size of FSTL5 detected with antibody A (94). To investigate if the protein sizes detected by the above three antibodies could be affected by caspase activities, INA-6 was treated in 0.1% BSA with different doses of Z-VAD-FMK, a pan-caspase inhibitor that could inhibit cleavage of

caspases and apoptosis. The 0.1% BSA medium contains fewer cell growth factors that could induce caspase-3 cleavage and cell death and the cleaved caspase-3 levels were taken as a positive control for validating the Z-VAD-FMK's effect. As shown in Fig. 16, cleaved caspase-3 could not be detected after treatment with Z-VAD-FMK, which indicated that the apoptosis pathway was inhibited.

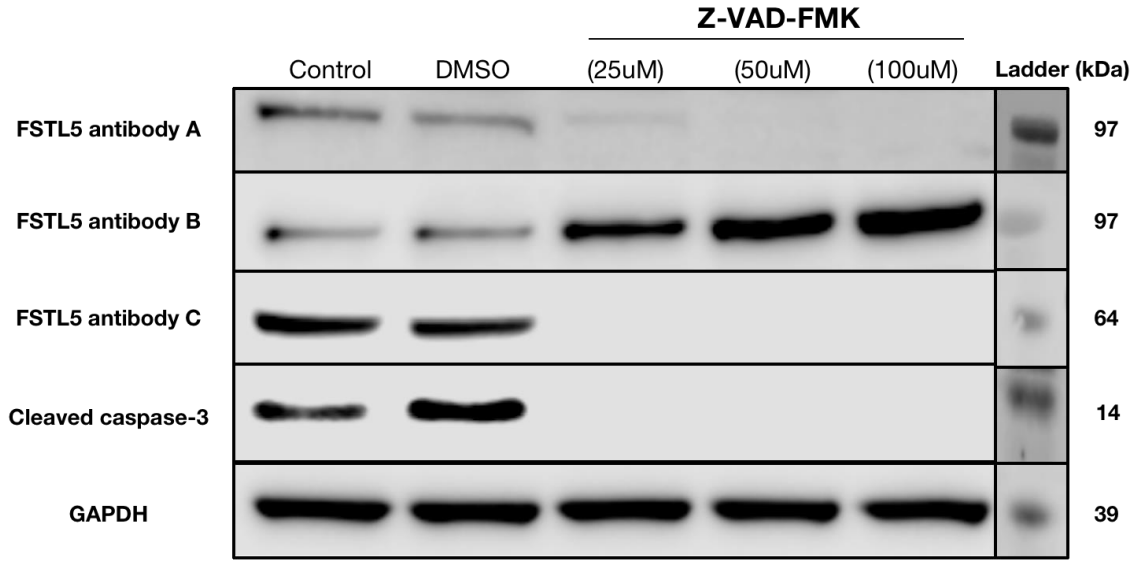

Figure 16. Effect of pan-caspase inhibitor on the sizes of the detected proteins in INA-6. Using INA-6 cells, 25 μM, 50 μM, and 100 μM of Z-VAD-FMK were tested along with dimethyl sulfoxide (DMSO), serving as a solvent control. The cells were cultured in 0.1% BSA (in RPMI) for 4 hours and western blot was performed thereafter by using FSTL5 antibody A, B, and E, with GAPDH antibody as the loading control. The figure represents one result of three repeats.

As seen before, the 97 kDa protein band detected with antibody A was reduced with the increase of Z-VAD-FMK doses and could not be detected when the concentration of Z-VAD-FMK reached to 50 μM (94). Whereas the 97 kDa protein detected with antibody B increased its amount with the increasing doses of Z-VAD-FMK. The 64 kDa protein displayed by antibody E could not be detected after treatment with Z-VAD-FMK. As for many of the other western blots, this result was confusing and we could not use it to conclude about antibody specificity. In summary, the proteins detected with antibody A and antibody E were decreased when the concentration of the pan-caspase inhibitor was increased, while the protein detected with antibody B was increased when the concentration of the inhibitor was increased.

4. Discussion

4.1 Expression of FSTL5 mRNA in different cell types and a panel of HMCLs

FSTL5 belongs to the follistatin-like family of genes whose functions are poorly understood. Due to alternative splicing, FSTL5 mRNA generates multiple transcript variants with different exon combinations (Fig. 2). To fully capture FSTL5 transcript variants, three pairs of primers towards different exon positions were applied in this project. From the RNA-seq data of human tissues in the Human Protein Atlas, FSTL5 mRNA is partially expressed in the human body and is especially enriched in the brain (32). Therefore, we included two brain organoids as potential positive controls and they were validated by the qRT-PCR results as well. In addition, the results also indicated that the brain-expressed transcripts contain at least exons 3-4, 6-7, and 15-16. In INA-6 cells, the failed amplification by FSTL5 primer pair 1 (exon 3-4) and primer pair 2 (exon 6-7) is in line with the previous results (94). However, we used FSTL5 primer pair 3 (exon 15-16) and first demonstrated that FSTL5 is expressed in INA-6 cells and that the expressed transcripts contain exon 15-16. The non-detectable or extremely high Ct values in Stroma, MSC, HEK 293, and HepG2 cell lines indicated low to no expression of these FSTL5 exons in them. However, two previous studies had found FSTL5 mRNA expressed in HepG2 cells (37,40). One possible explanation could be that they used FSTL5 primers towards different exons from ours and that those exons might be expressed in HepG2 cells (40). In addition, some methodology differences regarding total RNA extraction, cDNA synthesis, as well as qRT-PCR may have effects on the final results. The different exon combinations in different cell types revealed a possible cell type-specific expression of FSTL5. The FSTL5 gene expresses different transcript variants in different cell types, and this might be related to the specific functions of these cells.

Bolomsky and colleagues had found that compared to normal plasma cells, FSTL5 expression levels were up-regulated in a subset of MGUS cells, myeloma cells, and HMCLs (42). To further compare FSTL5 mRNA levels in HMCLs, qRT-PCR was performed in ten HMCLs. Since both results from us and the former master student (94) showed that the FSTL5 primer pair 1 and primer pair 2 did not work in several HMCLs, in this section, only FSTL5 primer pair 3 was applied. The qRT-PCR results revealed that VOLIN had a relatively high

FSTL5 expression level among the HMCLs, although with a big internal variation. This might be due to the less standardized growth of VOLIN cells. The VOLIN cells grow very slowly and seem to have a high turnover with a high rate of apoptotic cells in the culture (9). KJON-1, INA-6, U-266, IH-1, and URVIN also demonstrated FSTL5 expression (amount decreased successively). Our expression results were consistent with both the FSTL5 RNA-seq data (Appendix 5) as well as the previous unpublished Nanostring data from our lab. The good correlation between different methods in measuring FSTL5 in transcript levels made the results more reliable. Taking all the qRT-PCR results together, we found that except for the two brain organoid controls (AGC 1 and AGC 15), FSTL5 is also expressed in HMCLs but with different exon combinations, which indicates a potential role in MM. But more cell lines (such as normal plasma cells and myeloma cells from patients) need to be included to draw a solid conclusion.

4.2 Rapid amplification and sequencing of FSTL5 cDNA 5' ends in INA-6

From the previous results, FSTL5 primers designed towards exon 3-4 and exon 6-7 failed to produce amplification products by PCR in INA-6 whereas primer from exon 15-16 succeeded. This prompted us to investigate the sequences of the 5' end of FSTL5 mRNA in INA-6 cells. In order to obtain the 5' end segments of FSTL5, 5'-RACE experiment was performed and two antisense primers towards different exons were applied. The sequencing results were aligned with three protein-coding FSTL5 transcripts (Appendix 6, Fig. 10C). When being compared with transcripts FSTL5-201 and FSTL5-202, both short primer products and long primer products showed complete deletion of exon 11. Since FSTL5-203 already lacks exon 11, the products' sequences fit better with it and we therefore chose FSTL5-203 as the comparison template. The exon number 11-15 in FSTL5-203 is equivalent to the exon 12-16 in FSTL5 gene (Fig. 2). The results suggested the possible existence of a new transcript variant of FSTL5 that has not been annotated yet. Unlike the other five FSTL5 transcripts, this one is composed of FSTL5 exon 7-10 and exon 12-16 (exon numbering was based on the FSTL5 gene). Basically, this explained what we observed in qRT-PCR of why primers towards the first few exons did not work. Interestingly, the detected transcript contained partial sequences of intron 6 in the beginning. One of the annotated FSTL5 transcript variants, FSTL5-204, also starts with an intron (Fig. 2) and it is a non-protein-coding transcript. Therefore, we do not know whether the new FSTL5 transcript in INA-6 encodes protein or not. The probable reason for the existence of intron 6 in the detected transcript is intron retention during alternative splicing. Some point mutations at splice donor or acceptor sites could lead to aberrant intron retention (96). Partial or full retention of particular introns in mature transcripts has been observed in many different

types of cancers (97). In addition, it has been found that in MM, the hotspot mutations in the spliceosome component SF3B1 could change the preference of 3' splice sites in several genes and lead to aberrant splicing that alters the MM transcriptome and promotes the progression of MM (98). Taken together, the retention of FSTL5 intron 6 might be associated with MM, however, how it contributes to disease progression remains unknown. Deletion of the whole exon 8 appeared in one of the products from FSTL5 short primer. Since this product was amplified by FSTL5 short primer which might not demonstrate the full length of it, it is difficult to determine if this deletion was due to mutation or it actually indicated another form of a transcript. In addition, several point mutations and frameshift mutations were detected in some products but none of them were published on Mutalyzer database (99), so they might arise from experimental procedures, rather than being originated from INA-6 cells. It is essential to characterize FSTL5 transcript variants when investigating FSTL5 expression in HMCLs. Except for RACE, another method to identify transcript variants is RNA-seq. Transcripts are reversely transcribed to cDNAs and sequenced in parallel by next-generation sequencers (100). However, the relative FSTL5 mRNA levels were demonstrated pretty well by qRT-PCR, thus the identification of FSTL5 transcript variants in the other nine HMCLs by RACE and RNA-seq was not carried out due to time limitations.

4.3 Comparison of FSTL5 antibodies and expression of their corresponding proteins in HMCLs

Examining FSTL5 protein levels is another way to show its expression in cells and tissues. Previous results in the group displayed a 97 kDa protein by antibody A, which was approximately the same size as the full-length FSTL5 (94). However, since we did not manage to detect the full-length transcript of FSTL5 in INA-6, it is likely that the previously detected protein bands do not represent FSTL5. Therefore, we decided to add five more FSTL5 antibodies that were raised with variant parts of FSTL5 as immunogen in our experiment to get a better understanding of the protein expression. To compare the detection abilities of different antibodies to see if they all display the same pattern of FSTL5, six antibodies were tested against different experimental conditions in the beginning (Appendix 3). Antibody A, B, D, and E displayed clear bands varied from different experimental conditions, which indicated a relatively nice detection ability. The two mouse polyclonal antibodies—antibody C and antibody F displayed blurry bands and smear which did not change with various conditions, suggesting their bad specificity in recognizing targets. The reason behind this might be that these antibodies were generated against the full-length FSTL5 protein with multiple epitopes,

increasing the chance of non-specific cross reactivities in which they recognize other proteins containing homologous epitopes. Furthermore, the expression patterns and protein molecular weights displayed by antibody B and antibody D were quite similar whereas antibody B showed even stronger and clearer bands, we thus included antibody B rather than antibody D to avoid heavy and unnecessary workload. Therefore, antibody A, B, and E were applied in the following experiments.

Given that the FSTL5 transcript variants expressed by HMCLs were undetermined, the size and isoform of FSTL5 proteins in them were thus unknown. Therefore, western blot was performed in ten HMCLs using the selected primary antibody A, B, and E. FSTL5 was predicted to be a secretory protein (33). By using SignalP 5.0 (101), a signal sequence of FSTL5 that could be cleaved between the position 20 and 21 of the amino acid chain was discovered (Appendix 1). In order to experimentally validate this, cells were additionally treated with PTI. In the western blot results from antibody A and antibody B, bands of around 97 kDa were detected, which fit with the predicted full-size protein. Antibody E displayed a 64 kDa band that varied similarly to that of antibody A. Both antibody A and antibody E showed protein amount increased in the presence of PTI, suggesting that the proteins detected by them might be secreted. However, the band displayed by antibody B gave an opposite result, with protein levels decreased in the presence of PTI. It is speculated that the protein detected with antibody B was not secreted and that it was different from those detected with antibody A and E. Additionally, none of the protein levels correlated with our mRNA results in HMCLs. There are two possibilities: one is that the proteins detected by these antibodies are not the real FSTL5; and if the proteins are suspected to be FSTL5, this could be due to some complicated post-transcriptional mechanisms that are not well characterized. However, we do not have sufficient evidence to determine which antibody displayed the real FSTL5 protein or none of them did. In the results of antibody A, the cell line RPMI-8226, U-266, and JJN-3 displayed weaker bands compared to the previous results (94). This could be interpreted by the addition of IL-6 in all cell lines' experiment medium regardless of several IL-6 independent cell lines (VOLIN, RPMI-8226, U-266, and JJN-3) in our experiment and the IL-6 changed some cellular functions that might be related to protein production in these IL-6 independent cells.

4.4 Genetic knockout and knockdown of FSTL5 in INA-6

To determine whether the bands displayed by antibody A, B, and E were from FSTL5 protein, validation strategies were conducted. Antibody validation is a proof of its specificity

in recognizing potential targets and its selectivity in binding to the targets in the presence of a mixture of heterogeneous proteins (102). Gene KO/KD samples serve as excellent negative controls in evaluating the specificity of antibodies in western blot (102). The absence of expected bands in the KO cell line compared to positive control is strong evidence for indicating antibody's specificity (102). Here in this project, two FSTL5 KO INA-6 clones respectively targeting at FSTL5 exon 5 and exon 8 were used. Two times of experiments were performed whereas the results were irreproducible (Appendix 4, Fig. 12), suggesting that the CRISPR/Cas9 system might not be well-established in these cells. Here we only discuss the one that had relatively better results. The 97 kDa protein detected with antibody B showed reduced amount in FSTL5 exon 5 KO cells. The 97 kDa and 64 kDa proteins respectively detected with antibody A and antibody E showed reduced amount in FSTL5 exon 8 KO cells. Considering the FSTL5 transcript expressed by INA-6 possibly transcribes from exon 7, the KO of exon 5 might not affect the translation of FSTL5 protein, and it thus indicated that FSTL5 exon 5 KO cell line was not a good negative control. Therefore, the results from antibody B might be unconvincing. We could not suspect that the proteins detected with antibody A and antibody E were FSTL5 either because of the bad reproducible results from the KO cell lines. In addition, FSTL5 exon 8 KO cells and the WT control cells were tested against different drug's and proteins' effect. The aims were to investigate the role of FSTL5 on cell viability and to test if FSTL5 could be an antagonist of TGF-β family proteins because other FSTL proteins were shown to antagonize TGF-β family members. The results revealed that a potential knockout of FSTL5 did not affect how these drug/proteins worked on myeloma cells. Based on the results, the clones we used may not be the real KO cell lines. Both of the two KO clones have to be sequenced for determining the real KO effect in the future. Since the KO experiment was not successful, we could not conclude anything based on these results.

Given that the KO results did not solve the problem, another validation strategy gene KD was applied. The transfection of siFSTL5 into INA-6 cells showed 50% reduction of FSTL5 mRNA levels, suggesting that the KD worked. Therefore, the results from FSTL5 KD cells were more reliable compared to KO cells. In western blot, the 97 kDa protein detected with antibody A and the 64 kDa protein detected with antibody E were suspected to be secretory proteins because they showed increased levels in the presence of PTI. Besides, the two proteins reduced in siFSTL5 compared to siControl, which correlated with the change of mRNA levels. However, the 97 kDa protein detected with antibody B was not secreted and it showed even increased levels in FSTL5 KD cells, so we speculated that the protein detected with antibody B

was not the FSTL5 expressed by INA-6. Li *et al* had knocked down FSTL5 in HCC cell lines and got a significantly decreased level of the full-size FSTL5 protein (40), whereas none of the protein levels were reduced significantly in our results. The reason behind this could be the low KD efficiency of transfecting siRNA into INA-6, therefore further optimization strategies need to be applied to make KD more efficient. Based on the above, both the 97 kDa protein detected with antibody A and 64 kDa protein detected with antibody E have the possibility to be the correct form of FSTL5 in INA-6. When translating the new transcript sequences from 5'-RACE into amino acid sequences by some bioinformatic tools, we got a polypeptide chain with the molecular weight predicted to be around 63 kDa, which fit very well with the protein displayed by antibody E. However, further investigation should be done to confirm it. Considering we still got a certain amount of FSTL5 KD cells, the function of FSTL5 was explored by using these cells. However, as with the KO clones, the potential FSTL5 gene KD did not influence the drug's and proteins' effect on myeloma cells either. Therefore, we speculate that FSTL5 might not antagonize BMPs or activins and it did not influence cell viability as well.

4.5 Influence of general caspase inhibitor on the potential FSTL5 protein sizes in INA-6

FSTL5 is predicted to be cleaved at specific sites (Appendix 1). Two proteins, PYCARD and WBP4, are found to combine with FSTL5 in high affinities (34,103). PYCARD, also known as ASC, is an adaptor protein involved in caspase activation during apoptosis (104). Whether FSTL5 could be cleaved by caspases is undetermined. F. Alemu Atire had found that the general caspase inhibitor could have an impact on the cleavage of the 97 kDa protein detected with antibody A (94). We obtained consistent results with his, and furthermore, we found that the 64 kDa protein detected with antibody E could also be influenced by the general caspase inhibitor. Since we do not have solid evidence to show the correct protein isoform of FSTL5, we can only say that the 97 kDa protein detected with antibody A and 64 kDa protein detected with antibody E were related to caspases activities.

5. Conclusion and future perspectives

As the gene FSTL5 is found to be especially expressed in myeloma cells compared to normal plasma cells and could have prognostic value in MM, it is important to understand how this gene is expressed and what function it has in MM. By investigating FSTL5 expression in a range of cell types, we showed that FSTL5 is expressed in brain tissue. We also detected transcripts containing exon boundary 15-16 but not exon 3-4 and 6-7 in HMCLs, whereas not in other cell types such as Stroma, MSC, HEK293, and HepG2. We looked further into this and discovered that one of the HMCLs expresses a novel FSTL5 transcript variant with unknown functions. Additionally, the expression of FSTL5 protein in HMCLs is still unclear, partly due to invalid antibodies. What's more, by using gene knockdown, we could not demonstrate any antagonizing effect of FSTL5 on BMP or activins and we could not see any effect on cell viability. Finally, no evidence showed that FSTL5 could be regulated by caspases.

This thesis had given a preliminary understanding of the expression and function of FSTL5 in MM, but further efforts could be done to investigate this gene more in-depth. First, it would be of interest to explore FSTL5 mRNA expression in more MM-related cells (such as MGUS cells, SMM cells, and myeloma cells from patients) to know if it is specific to MM. In addition, it is also adoptable to set a positive control for western blot with cells already known to express FSTL5 protein (e.g. brain tissue) and compare more FSTL5 antibodies to get much more trustable results. Given that the predicted molecular weight of the translated new transcript fits with the size of the protein band detected with antibody E (catalog number: NBP2-14028), it is therefore needed to investigate whether they are the same protein. One way is to construct an expression vector containing reversely transcribed DNA sequences from the detected transcript, and express it in INA-6. If the expression system could produce recombinant protein, then western blot can be performed to check if the protein displays the same band by antibody E. Besides, one could also express the transcript in myeloma cell lines and perform various functional assays (e.g. cell viability, proliferation, and migration) to explore its function in MM.

References

1. Mitsiades CS, Mitsiades N, Munshi NC, Anderson KC. Focus on multiple myeloma. Cancer Cell. 2004;6(5):439–44.
2. Anderson KC, Alsina M, Bensinger W, Biermann JS, Chanan-Khan A, Cohen AD, et al. Multiple myeloma. J Natl Compr Cancer Netw. 2009;7(9):908–42.
3. Bergsagel PL, Kuehl WM. Chromosome translocations in multiple myeloma [Internet]. [cited 2021 May 13]. Available from: www.nature.com/onc
4. Kyle RA, Vincent Rajkumar S. Multiple Myeloma [Internet]. Vol. 18, N Engl J Med. 2004. Available from: www.nejm.org
5. Becker N. Epidemiology of multiple myeloma. Mult myeloma. 2011;25–35.
6. Kyle RA, Rajkumar SV. Treatment of multiple myeloma: a comprehensive review. Clin Lymphoma Myeloma. 2009;9(4):278–88.
7. Attal M, Harousseau J-L, Stoppa A-M, Sotto J-J, Fuzibet J-G, Rossi J-F, et al. A prospective, randomized trial of autologous bone marrow transplantation and chemotherapy in multiple myeloma. N Engl J Med. 1996;335(2):91–7.
8. Kumar A, Loughran T, Alsina M, Durie BGM, Djulbegovic B. Management of multiple myeloma: a systematic review and critical appraisal of published studies. Lancet Oncol. 2003;4(5):293–304.
9. Våtsveen TK, Børset M, Dikic A, Tian E, Micci F, Lid AHB, et al. VOLIN and KJON—Two novel hyperdiploid myeloma cell lines. Genes, Chromosom Cancer. 2016;55(11):890–901.
10. Moreaux J, Klein B, Bataille R, Descamps G, Maïga S, Hose D, et al. A high-risk signature for patients with multiple myeloma established from the molecular classification of human myeloma cell lines. Haematologica. 2011;96(4):574.
11. Hinck AP. Structural studies of the TGF-βs and their receptors–insights into evolution of the TGF-β superfamily. FEBS Lett. 2012;586(14):1860–70.
12. Heldin C-H, Moustakas A. Signaling receptors for TGF-β family members. Cold Spring Harb Perspect Biol. 2016;8(8):a022053.
13. Mahindra A, Hideshima T, Anderson KC. Multiple myeloma: biology of the disease. Blood Rev. 2010;24:S5–11.
14. Holien T, Våtsveen TK, Hella H, Rampa C, Brede G, Grøseth LAG, et al. Bone morphogenetic proteins induce apoptosis in multiple myeloma cells by Smad-dependent repression of MYC. Leukemia. 2012;26(5):1073–80.

15. Holien T, Sundan A. The role of bone morphogenetic proteins in myeloma cell survival. Cytokine Growth Factor Rev. 2014;25(3):343–50.
16. Vallet S, Mukherjee S, Vaghela N, Hideshima T, Fulciniti M, Pozzi S, et al. Activin A promotes multiple myeloma-induced osteolysis and is a promising target for myeloma bone disease. Proc Natl Acad Sci. 2010;107(11):5124–9.
17. Olsen OE, Wader KF, Hella H, Mylin AK, Turesson I, Nesthus I, et al. Activin A inhibits BMP-signaling by binding ACVR2A and ACVR2B. Cell Commun Signal. 2015;13(1):1–7.
18. Keutmann HT, Schneyer AL, Sidis Y. The role of follistatin domains in follistatin biological action. Mol Endocrinol. 2004;18(1):228–40.
19. Tian M, Kamoun S. A two disulfide bridge Kazal domain from Phytophthora exhibits stable inhibitory activity against serine proteases of the subtilisin family. BMC Biochem. 2005;6(1):1–9.
20. Sylva M, Moorman AFM, Van den Hoff MJB. Follistatin-like 1 in vertebrate development. Birth Defects Res Part C Embryo Today Rev. 2013;99(1):61–9.
21. Oshima Y, Ouchi N, Sato K, Izumiya Y, Pimentel DR, Walsh K. Follistatin-like 1 is an Akt-regulated cardioprotective factor that is secreted by the heart. Circulation. 2008;117(24):3099.
22. Wei K, Serpooshan V, Hurtado C, Diez-Cunado M, Zhao M, Maruyama S, et al. Epicardial FSTL1 reconstitution regenerates the adult mammalian heart. Nature. 2015;525(7570):479–85.
23. Trojan L, Schaaf A, Steidler A, Haak M, Thalmann G, Knoll T, et al. Identification of metastasis-associated genes in prostate cancer by genetic profiling of human prostate cancer cell lines. Anticancer Res. 2005;25(1A):183–91.
24. Fainsod A, Deißler K, Yelin R, Marom K, Epstein M, Pillemer G, et al. The dorsalizing and neural inducing gene follistatin is an antagonist of BMP-4. Mech Dev. 1997;63(1):39–50.
25. Hardy CL, Nguyen H-A, Mohamud R, Yao J, Oh DY, Plebanski M, et al. The activin A antagonist follistatin inhibits asthmatic airway remodelling. Thorax. 2013;68(1):9–18.
26. Glister C, Kemp CF, Knight PG. Bone morphogenetic protein (BMP) ligands and receptors in bovine ovarian follicle cells: actions of BMP-4,-6 and-7 on granulosa cells and differential modulation of Smad-1 phosphorylation by follistatin. Reproduction. 2004;127(2):239–54.

27. Geng Y, Dong Y, Yu M, Zhang L, Yan X, Sun J, et al. Follistatin-like 1 (Fstl1) is a bone morphogenetic protein (BMP) 4 signaling antagonist in controlling mouse lung development. Proc Natl Acad Sci. 2011;108(17):7058–63.
28. Sidis Y, Mukherjee A, Keutmann H, Delbaere A, Sadatsuki M, Schneyer A. Biological activity of follistatin isoforms and follistatin-like-3 is dependent on differential cell surface binding and specificity for activin, myostatin, and bone morphogenetic proteins. Endocrinology. 2006;147(7):3586–97.
29. Massagué J, Chen Y-G. Controlling TGF-β signaling. Genes Dev. 2000;14(6):627–44.
30. Team MGC (MGC) P. Generation and initial analysis of more than 15,000 full-length human and mouse cDNA sequences. Proc Natl Acad Sci. 2002;99(26):16899–903.
31. Howe KL, Achuthan P, Allen J, Allen J, Alvarez-Jarreta J, Amode MR, et al. Ensembl 2021. Nucleic Acids Res [Internet]. 2021;49(2). Available from: https://www.ncbi.nlm.nih.gov/dbvar/studies/nstd186
32. Uhlén M, Fagerberg L, Hallström BM, Lindskog C, Oksvold P, Mardinoglu A, et al. Tissue-based map of the human proteome [Internet]. Science. 2015 [cited 2021 Apr 21]. Available from: http://science.sciencemag.org/
33. Masuda T, Sakuma C, Nagaoka A, Yamagishi T, Ueda S, Nagase T, et al. F ollistatin-like 5 is expressed in restricted areas of the adult mouse brain: Implications for its function in the olfactory system. Congenit Anom (Kyoto). 2014;54(1):63–6.
34. Dowling JK, Becker CE, Bourke NM, Corr SC, Connolly DJ, Quinn SR, et al. Promyelocytic leukemia protein interacts with the apoptosis-associated speck-like protein to limit inflammasome activation. J Biol Chem. 2014;289(10):6429–37.
35. Zabala W, Cruz R, Barreiro-de Acosta M, Chaparro M, Panes J, Echarri A, et al. New genetic associations in thiopurine-related bone marrow toxicity among inflammatory bowel disease patients. Pharmacogenomics. 2013;14(6):631–40.
36. Remke M, Hielscher T, Korshunov A, Northcott PA, Bender S, Kool M, et al. FSTL5 is a marker of poor prognosis in non-WNT/non-SHH medulloblastoma. J Clin Oncol. 2011;29(29):3852–61.
37. Zhang D, Ma X, Sun W, Cui P, Lu Z. Down-regulated FSTL5 promotes cell proliferation and survival by affecting Wnt/β-catenin signaling in hepatocellular carcinoma. Int J Clin Exp Pathol. 2015;8(3):3386.
38. Zhang D-Y, Sun W-L, Ma X, Zhang P, Wu W, Wu H, et al. Up-regulated FSTL5 inhibits invasion of hepatocellular carcinoma through the Wnt/β-catenin/YAP pathway. Int J Clin Exp Pathol. 2017;10(10):10325.

39. Zhang D-Y, Lei J-S, Sun W-L, Wang D-D, Lu Z. Follistatin Like 5 (FSTL5) inhibits epithelial to mesenchymal transition in hepatocellular carcinoma. Chin Med J (Engl). 2020;133(15):1798.
40. Li C, Dai L, Zhang J, Zhang Y, Lin Y, Cheng L, et al. Follistatin-like protein 5 inhibits hepatocellular carcinoma progression by inducing caspase-dependent apoptosis and regulating Bcl-2 family proteins. J Cell Mol Med. 2018;22(12):6190–201.
41. Rosell R, Karachaliou N, Codony-Servat C, Ito M. Inhibition of MEK, a canonical KRAS pathway effector in KRAS mutant NSCLC. Transl lung cancer Res. 2018;7(Suppl 3):S183.
42. Bolomsky A, Hose D, Schreder M, Seckinger A, Lipp S, Klein B, et al. Insulin like growth factor binding protein 7 (IGFBP7) expression is linked to poor prognosis but may protect from bone disease in multiple myeloma. J Hematol Oncol. 2015;8(1):1–14.
43. Shyu A, Wilkinson MF, Van Hoof A. Messenger RNA regulation: to translate or to degrade. EMBO J. 2008;27(3):471–81.
44. Matoulkova E, Michalova E, Vojtesek B, Hrstka R. The role of the 3'untranslated region in post-transcriptional regulation of protein expression in mammalian cells. RNA Biol. 2012;9(5):563–76.
45. van den Hoogenhof MMG, Pinto YM, Creemers EE. RNA splicing: regulation and dysregulation in the heart. Circ Res. 2016;118(3):454–68.
46. Kim E, Goren A, Ast G. Alternative splicing: current perspectives. Bioessays. 2008;30(1):38–47.
47. Zheng CL, Fu X-D, Gribskov M. Characteristics and regulatory elements defining constitutive splicing and different modes of alternative splicing in human and mouse. Rna. 2005;11(12):1777–87.
48. Matlin AJ, Clark F, Smith CWJ. Understanding alternative splicing: towards a cellular code. Nat Rev Mol cell Biol. 2005;6(5):386–98.
49. de la Mata M, Alonso CR, Kadener S, Fededa JP, Blaustein M, Pelisch F, et al. A slow RNA polymerase II affects alternative splicing in vivo. Mol Cell. 2003;12(2):525–32.
50. Wang Y, Liu J, Huang BO, Xu Y, Li J, Huang L, et al. Mechanism of alternative splicing and its regulation. Biomed reports. 2015;3(2):152–8.
51. Wang Z, Burge CB. Splicing regulation: from a parts list of regulatory elements to an integrated splicing code. Rna. 2008;14(5):802–13.
52. Cieply B, Carstens RP. Functional roles of alternative splicing factors in human disease. Wiley Interdiscip Rev RNA. 2015;6(3):311–26.

53. Shenasa H, Hertel KJ. Combinatorial regulation of alternative splicing. Biochim Biophys Acta (BBA)-Gene Regul Mech. 2019;1862(11–12):194392.
54. Erkelenz S, Mueller WF, Evans MS, Busch A, Schöneweis K, Hertel KJ, et al. Position-dependent splicing activation and repression by SR and hnRNP proteins rely on common mechanisms. Rna. 2013;19(1):96–102.
55. Misteli T, Spector DL. RNA polymerase II targets pre-mRNA splicing factors to transcription sites in vivo. Mol Cell. 1999;3(6):697–705.
56. Zhu L-Y, Zhu Y-R, Dai D-J, Wang X, Jin H-C. Epigenetic regulation of alternative splicing. Am J Cancer Res. 2018;8(12):2346.
57. Faustino NA, Cooper TA. Pre-mRNA splicing and human disease. Genes Dev. 2003;17(4):419–37.
58. Garcia-Blanco MA, Baraniak AP, Lasda EL. Alternative splicing in disease and therapy. Nat Biotechnol. 2004;22(5):535–46.
59. Singh B, Eyras E. The role of alternative splicing in cancer. Transcription. 2017;8(2):91–8.
60. Bechara EG, Sebestyén E, Bernardis I, Eyras E, Valcárcel J. RBM5, 6, and 10 differentially regulate NUMB alternative splicing to control cancer cell proliferation. Mol Cell. 2013;52(5):720–33.
61. Ghigna C, Giordano S, Shen H, Benvenuto F, Castiglioni F, Comoglio PM, et al. Cell motility is controlled by SF2/ASF through alternative splicing of the Ron protooncogene. Mol Cell. 2005;20(6):881–90.
62. Trincado JL, Sebestyen E, Pages A, Eyras E. The prognostic potential of alternative transcript isoforms across human tumors. Genome Med. 2016;8(1):1–14.
63. Zhang Z, Henzel WJ. Signal peptide prediction based on analysis of experimentally verified cleavage sites. Protein Sci. 2004;13(10):2819–24.
64. Nakai K. Protein sorting signals and prediction of subcellular localization. Adv Protein Chem. 2000;54:277–344.
65. Blobel G, Dobberstein B. Transfer of proteins across membranes. I. Presence of proteolytically processed and unprocessed nascent immunoglobulin light chains on membrane-bound ribosomes of murine myeloma. J Cell Biol. 1975;67(3):835–51.
66. Paetzel M, Karla A, Strynadka NCJ, Dalbey RE. Signal peptidases. Chem Rev. 2002;102(12):4549–80.
67. Chowdhury I, Tharakan B, Bhat GK. Caspases—an update. Comp Biochem Physiol Part B Biochem Mol Biol. 2008;151(1):10–27.

68. Bao Y, Marini S, Tamura T, Kamada M, Maegawa S, Hosokawa H, et al. Toward more accurate prediction of caspase cleavage sites: a comprehensive review of current methods, tools and features. Brief Bioinform. 2019;20(5):1669–84.
69. Pop C, Salvesen GS. Human caspases: activation, specificity, and regulation. J Biol Chem. 2009;284(33):21777–81.
70. Hjertner O, Hjorth-Hansen H, Börset M, Seidel C, Waage A, Sundan A. Bone morphogenetic protein-4 inhibits proliferation and induces apoptosis of multiple myeloma cells: Presented in part at the 41st annual meeting of the American Society of Hematology, New Orleans, December 1999. Blood, J Am Soc Hematol. 2001;97(2):516–22.
71. Börset M, Waage A, Brekke OL, Helseth E. TNF and IL-6 are potent growth factors for OH-2, a novel human myeloma cell line. Eur J Haematol. 1994;53(1):31–7.
72. Matsuoka Y, Moore GE, Yagi Y, Pressman D. Production of free light chains of immunoglobulin by a hematopoietic cell line derived from a patient with multiple myeloma. Proc Soc Exp Biol Med. 1967;125(4):1246–50.
73. Nilsson K, Bennich H, Johansson SGO, Ponten J. Established immunoglobulin producing myeloma (IgE) and lymphoblastoid (IgG) cell lines from an IgE myeloma patient. Clin Exp Immunol. 1970;7(4):477.
74. Burger R, Guenther A, Bakker F, Schmalzing M, Bernand S, Baum W, et al. Gp130 and ras mediated signaling in human plasma cell line INA-6: a cytokine-regulated tumor model for plasmacytoma. Hematol J. 2001;2(1):42–53.
75. Jelinek DF, Ahmann GJ, Greipp PR, Jalal SM, Westendorf JJ, Katzmann JA, et al. Coexistence of aneuploid subclones within a myeloma cell line that exhibits clonal immunoglobulin gene rearrangement: clinical implications. Cancer Res. 1993;53(21):5320–7.
76. Jackson N, Lowe J, Ball J, Bromidge E, Ling NR, Larkins S, et al. Two new IgA1-kappa plasma cell leukaemia cell lines (JJN-1 & JJN-2) which proliferate in response to B cell stimulatory factor 2. Clin Exp Immunol. 1989;75(1):93.
77. Harrington AE, Morris-Triggs SA, Ruotolo BT, Robinson C V, Ohnuma S, Hyvönen M. Structural basis for the inhibition of activin signalling by follistatin. EMBO J. 2006;25(5):1035–45.
78. Schochetman G, Ou C-Y, Jones WK. Polymerase chain reaction. J Infect Dis. 1988;158(6):1154–7.
79. Freeman WM, Walker SJ, Vrana KE. Quantitative RT-PCR: pitfalls and potential. Biotechniques. 1999;26(1):112–25.

80. Kutyavin I V, Afonina IA, Mills A, Gorn V V, Lukhtanov EA, Belousov ES, et al. 3′-minor groove binder-DNA probes increase sequence specificity at PCR extension temperatures. Nucleic Acids Res. 2000;28(2):655–61.
81. Frohman MA. On beyond classic RACE (rapid amplification of cDNA ends). Genome Res. 1994;4(1):S40–58.
82. Takara Bio. SMARTer ® RACE 5 ’/ 3 ’ Kit User Manual [Internet]. [cited 2021 Apr 20]. Available from: https://www.takarabio.com/documents/User Manual/SMARTer RACE 5%273%27 Kit User Manual/SMARTer RACE 5%273%27 Kit User Manual_052617.pdf
83. Hnasko TS, Hnasko RM. The western blot. In: ELISA. Springer; 2015. p. 87–96.
84. Alegria-Schaffer A, Lodge A, Vattem K. Performing and optimizing Western blots with an emphasis on chemiluminescent detection. Methods Enzymol. 2009;463:573–99.
85. Ghosh R, Gilda JE, Gomes A V. The necessity of and strategies for improving confidence in the accuracy of western blots. Expert Rev Proteomics. 2014;11(5):549–60.
86. Tomari Y, Zamore PD. Perspective: machines for RNAi. Genes Dev. 2005;19(5):517–29.
87. Laganà A, Veneziano D, Russo F, Pulvirenti A, Giugno R, Croce CM, et al. Computational design of artificial RNA molecules for gene regulation. In: RNA Bioinformatics. Springer; 2015. p. 393–412.
88. Tang G. siRNA and miRNA: an insight into RISCs. Trends Biochem Sci. 2005;30(2):106–14.
89. Fagerli U-M, Holt RU, Holien T, Vaatsveen TK, Zhan F, Egeberg KW, et al. Overexpression and involvement in migration by the metastasis-associated phosphatase PRL-3 in human myeloma cells. Blood, J Am Soc Hematol. 2008;111(2):806–15.
90. Promega. CellTiter-Glo 2.0 Assay - Technical Manual [Internet]. Promega. 2017 [cited 2021 May 10]. p. 17. Available from: https://no.promega.com/-/media/files/resources/protocols/technical-manuals/101/celltiterglo-2-0-assay-protocol.pdf?la=en
91. Crouch SPM, Kozlowski R, Slater KJ, Fletcher J. The use of ATP bioluminescence as a measure of cell proliferation and cytotoxicity. J Immunol Methods. 1993;160(1):81–8.
92. Bookout AL, Mangelsdorf DJ, Hughes H. Quantitative real-time PCR protocol for analysisof nuclear receptor signaling pathways. Nucl Recept Signal [Internet]. 2003;1:12. Available from: www.nursa.org
93. Jonathan J Keats. FSTL5 Gene Expression [Internet]. [cited 2021 May 20]. Available from: https://www.keatslab.org/

94. Atire FA. Expression and regulation of FSTL5 in multiple myeloma cells. Unpublished. Norwegian University of Science and Technology; 2017.
95. ThermoFisher Scientific. Technical Data Sheet: Protein Transport Inhibitor Cocktail (500X) [Internet]. [cited 2021 May 20]. Available from: https://www.thermofisher.com/document-connect/document-connect.html?url=https://assets.thermofisher.com/TFS-Assets/LSG/manuals/00-4980.pdf
96. Wong JJ, Au AYM, Ritchie W, Rasko JEJ. Intron retention in mRNA: No longer nonsense: Known and putative roles of intron retention in normal and disease biology. Bioessays. 2016;38(1):41–9.
97. Dvinge H, Bradley RK. Widespread intron retention diversifies most cancer transcriptomes. Genome Med. 2015;7(1):1–13.
98. Bauer MA, Ashby C, Wardell C, Boyle EM, Ortiz M, Flynt E, et al. Differential RNA splicing as a potentially important driver mechanism in multiple myeloma. Haematologica. 2021;106(3):736.
99. Lefter M, Vis JK, Vermaat M, Den Dunnen JT, Taschner PEM, Laros JFJ, et al. Subject Section Mutalyzer 2 Next Generation HGVS Nomenclature Checker. Available from: https://academic.oup.com/bioinformatics/advance-article/doi/10.1093/bioinformatics/btab051/6128506
100. Weirick T, Militello G, Müller R, John D, Dimmeler S, Uchida S. The identification and characterization of novel transcripts from RNA-seq data. Brief Bioinform. 2016;17(4):678–85.
101. Juan J, Armenteros A, Tsirigos KD, Sønderby CK, Petersen TN, Winther O, et al. Brief CommuniCation SignalP 5.0 improves signal peptide predictions using deep neural networks [Internet]. Vol. 37, NATure BiOTeCHNOlOGy |. 2019 [cited 2021 May 20]. Available from: http://www.cbs.dtu.dk/services/SignalP/
102. Pillai-Kastoori L, Heaton S, Shiflett SD, Roberts AC, Solache A, Schutz-Geschwender AR. Antibody validation for Western blot: by the user, for the user. J Biol Chem. 2020;295(4):926–39.
103. Huttlin EL, Bruckner RJ, Paulo JA, Cannon JR, Ting L, Baltier K, et al. Architecture of the human interactome defines protein communities and disease networks. Nature. 2017;545(7655):505–9.
104. Rossi MN, Antonangeli F. LncRNAs: new players in apoptosis control. Int J Cell Biol. 2014;2014.

Appendices

Appendix 1: Predicted signal peptide and cleavage site of FSTL5 protein isoforms.

Appendix 2: Alignment of nucleotide sequences of 5'-RACE products.

Appendix 3: Comparison of different antibodies' performances.

Appendix 4: Validation of antibodies with FSTL5 KO cells.

Appendix 5: Expression of FSTL5 across eight HMCLs by RNA-seq.

Appendix 6: Sequence alignments with FSTL5 transcript variants.

Appendix 1: Predicted signal peptide and cleavage site of FSTL5 protein isoforms. A) Protein sequences translated from FSTL5-201. B) Protein sequences translated from FSTL5-202. C) Protein sequences translated from FSTL5-203. The red solid lines represent FSTL5 signal peptide sequences, the peaks of green dotted lines demonstrate the cleavage site position, and the orange dotted lines represent mature protein sequences.

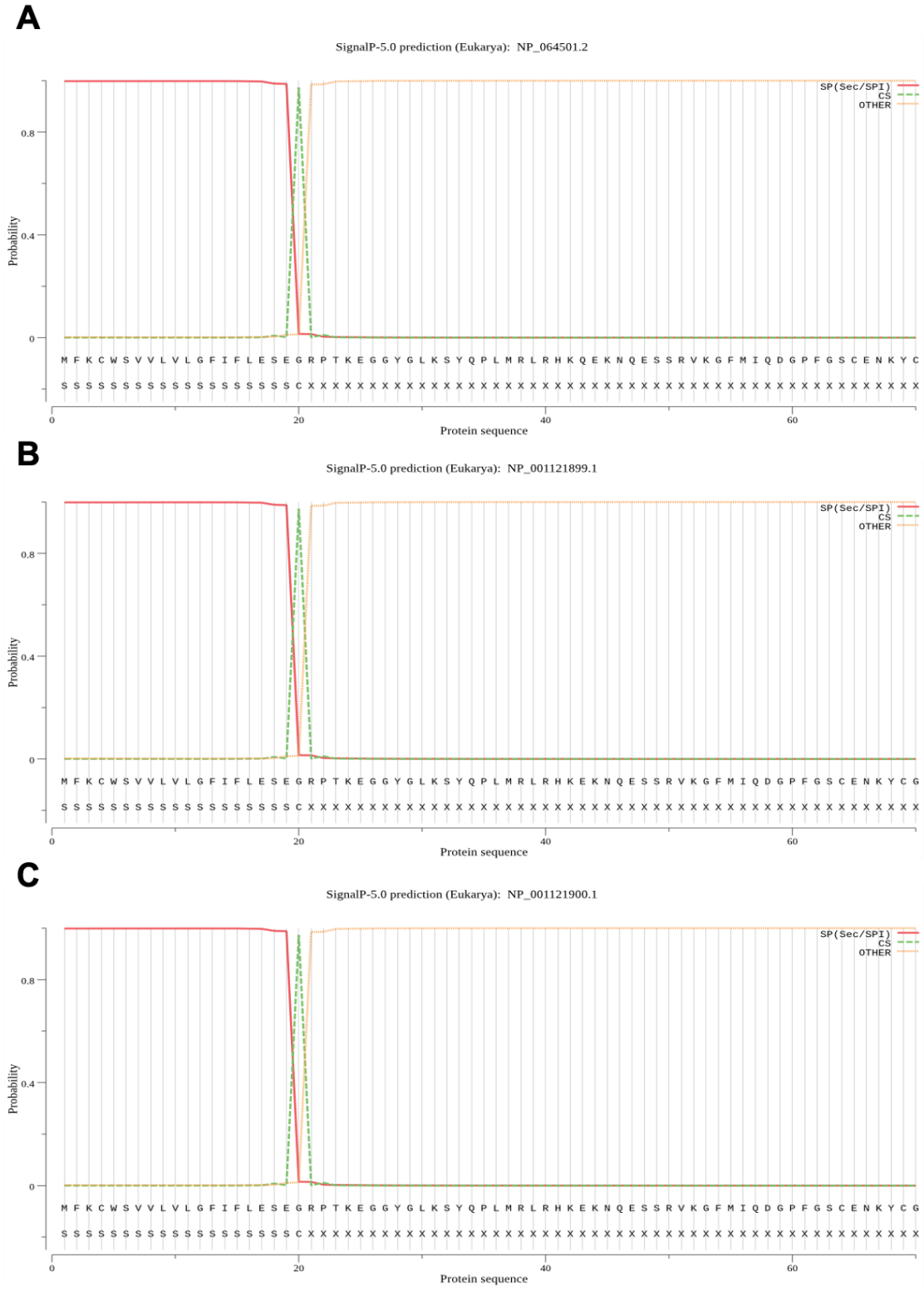

Appendix 2: Alignment of nucleotide sequences of 5'-RACE products. The detailed sequencing results of both FSTL5 short primer products (A) and FSTL5 long primer products (B) were aligned with FSTL5-203. The positions of intron or exons were shown by arrows. The nucleotides colored with green represent the sequences from intron 6 and the sequences colored with orange represent FSTL5 short/long primers. Mutated positions were indicated with the red and bold font.

A

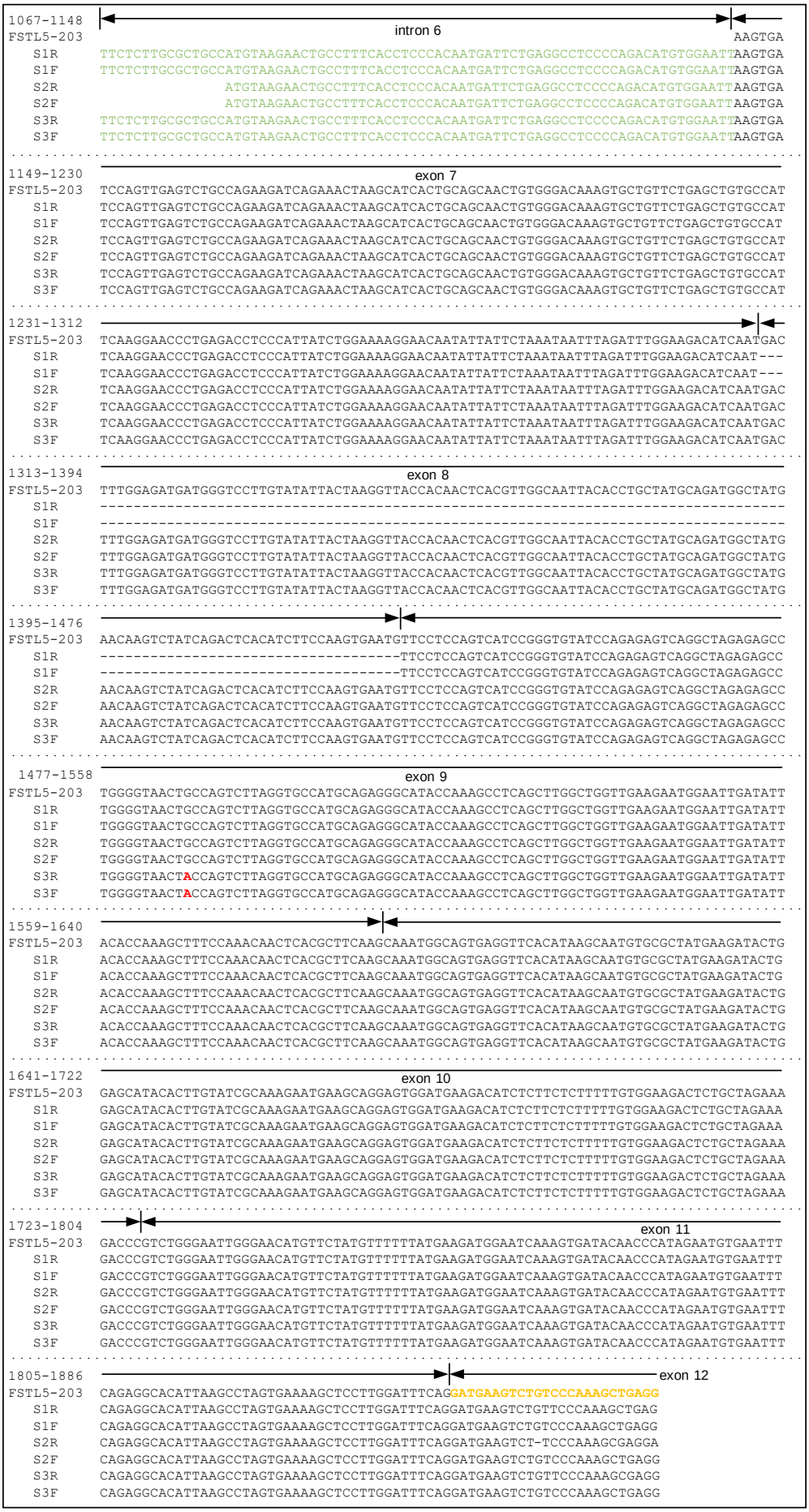
1067-1148
intron 6
FSTL5-203 AAGTGA
S1R TTCTCTTGCGCTGCCATGTAAGAACTGCCTTTCACCTCCCACAATGATTCTGAGGCCTCCCCAGACATGTGGAATTAAGTGA
S1F TTCTCTTGCGCTGCCATGTAAGAACTGCCTTTCACCTCCCACAATGATTCTGAGGCCTCCCCAGACATGTGGAATTAAGTGA
S2R ATGTAAGAACTGCCTTTCACCTCCCACAATGATTCTGAGGCCTCCCCAGACATGTGGAATTAAGTGA
S2F ATGTAAGAACTGCCTTTCACCTCCCACAATGATTCTGAGGCCTCCCCAGACATGTGGAATTAAGTGA
S3R TTCTCTTGCGCTGCCATGTAAGAACTGCCTTTCACCTCCCACAATGATTCTGAGGCCTCCCCAGACATGTGGAATTAAGTGA
S3F TTCTCTTGCGCTGCCATGTAAGAACTGCCTTTCACCTCCCACAATGATTCTGAGGCCTCCCCAGACATGTGGAATTAAGTGA
1149-1230
exon 7
FSTL5-203 TCCAGTTGAGTCTGCCAGAAGATCAGAAACTAAGCATCACTGCAGCAACTGTGGGACAAAGTGCTGTTCTGAGCTGTGCCAT
S1R TCCAGTTGAGTCTGCCAGAAGATCAGAAACTAAGCATCACTGCAGCAACTGTGGGACAAAGTGCTGTTCTGAGCTGTGCCAT
S1F TCCAGTTGAGTCTGCCAGAAGATCAGAAACTAAGCATCACTGCAGCAACTGTGGGACAAAGTGCTGTTCTGAGCTGTGCCAT
S2R TCCAGTTGAGTCTGCCAGAAGATCAGAAACTAAGCATCACTGCAGCAACTGTGGGACAAAGTGCTGTTCTGAGCTGTGCCAT
S2F TCCAGTTGAGTCTGCCAGAAGATCAGAAACTAAGCATCACTGCAGCAACTGTGGGACAAAGTGCTGTTCTGAGCTGTGCCAT
S3R TCCAGTTGAGTCTGCCAGAAGATCAGAAACTAAGCATCACTGCAGCAACTGTGGGACAAAGTGCTGTTCTGAGCTGTGCCAT
S3F TCCAGTTGAGTCTGCCAGAAGATCAGAAACTAAGCATCACTGCAGCAACTGTGGGACAAAGTGCTGTTCTGAGCTGTGCCAT
1231-1312
FSTL5-203 TCAAGGAACCCTGAGACCTCCCATTATCTGGAAAAGGAACAATATTATTCTAAATAATTTAGATTTGGAAGACATCAATGAC
S1R TCAAGGAACCCTGAGACCTCCCATTATCTGGAAAAGGAACAATATTATTCTAAATAATTTAGATTTGGAAGACATCAAT---
S1F TCAAGGAACCCTGAGACCTCCCATTATCTGGAAAAGGAACAATATTATTCTAAATAATTTAGATTTGGAAGACATCAAT---
S2R TCAAGGAACCCTGAGACCTCCCATTATCTGGAAAAGGAACAATATTATTCTAAATAATTTAGATTTGGAAGACATCAATGAC
S2F TCAAGGAACCCTGAGACCTCCCATTATCTGGAAAAGGAACAATATTATTCTAAATAATTTAGATTTGGAAGACATCAATGAC
S3R TCAAGGAACCCTGAGACCTCCCATTATCTGGAAAAGGAACAATATTATTCTAAATAATTTAGATTTGGAAGACATCAATGAC
S3F TCAAGGAACCCTGAGACCTCCCATTATCTGGAAAAGGAACAATATTATTCTAAATAATTTAGATTTGGAAGACATCAATGAC
1313-1394
exon 8
FSTL5-203 TTTGGAGATGATGGGTCCTTGTATATTACTAAGGTTACCACAACTCACGTTGGCAATTACACCTGCTATGCAGATGGCTATG
S1R ----------
S1F ----------
S2R TTTGGAGATGATGGGTCCTTGTATATTACTAAGGTTACCACAACTCACGTTGGCAATTACACCTGCTATGCAGATGGCTATG
S2F TTTGGAGATGATGGGTCCTTGTATATTACTAAGGTTACCACAACTCACGTTGGCAATTACACCTGCTATGCAGATGGCTATG
S3R TTTGGAGATGATGGGTCCTTGTATATTACTAAGGTTACCACAACTCACGTTGGCAATTACACCTGCTATGCAGATGGCTATG
S3F TTTGGAGATGATGGGTCCTTGTATATTACTAAGGTTACCACAACTCACGTTGGCAATTACACCTGCTATGCAGATGGCTATG
1395-1476
FSTL5-203 AACAAGTCTATCAGACTCACATCTTCCAAGTGAATGTTCCTCCAGTCATCCGGGTGTATCCAGAGAGTCAGGCTAGAGAGCC
S1R ----------TTCCTCCAGTCATCCGGGTGTATCCAGAGAGTCAGGCTAGAGAGCC
S1F ----------TTCCTCCAGTCATCCGGGTGTATCCAGAGAGTCAGGCTAGAGAGCC
S2R AACAAGTCTATCAGACTCACATCTTCCAAGTGAATGTTCCTCCAGTCATCCGGGTGTATCCAGAGAGTCAGGCTAGAGAGCC
S2F AACAAGTCTATCAGACTCACATCTTCCAAGTGAATGTTCCTCCAGTCATCCGGGTGTATCCAGAGAGTCAGGCTAGAGAGCC
S3R AACAAGTCTATCAGACTCACATCTTCCAAGTGAATGTTCCTCCAGTCATCCGGGTGTATCCAGAGAGTCAGGCTAGAGAGCC
S3F AACAAGTCTATCAGACTCACATCTTCCAAGTGAATGTTCCTCCAGTCATCCGGGTGTATCCAGAGAGTCAGGCTAGAGAGCC
1477-1558
exon 9
FSTL5-203 TGGGGTAACTGCCAGTCTTAGGTGCCATGCAGAGGGCATACCAAAGCCTCAGCTTGGCTGGTTGAAGAATGGAATTGATATT
S1R TGGGGTAACTGCCAGTCTTAGGTGCCATGCAGAGGGCATACCAAAGCCTCAGCTTGGCTGGTTGAAGAATGGAATTGATATT
S1F TGGGGTAACTGCCAGTCTTAGGTGCCATGCAGAGGGCATACCAAAGCCTCAGCTTGGCTGGTTGAAGAATGGAATTGATATT
S2R TGGGGTAACTGCCAGTCTTAGGTGCCATGCAGAGGGCATACCAAAGCCTCAGCTTGGCTGGTTGAAGAATGGAATTGATATT
S2F TGGGGTAACTGCCAGTCTTAGGTGCCATGCAGAGGGCATACCAAAGCCTCAGCTTGGCTGGTTGAAGAATGGAATTGATATT
S3R TGGGGTAACTACCAGTCTTAGGTGCCATGCAGAGGGCATACCAAAGCCTCAGCTTGGCTGGTTGAAGAATGGAATTGATATT
S3F TGGGGTAACTACCAGTCTTAGGTGCCATGCAGAGGGCATACCAAAGCCTCAGCTTGGCTGGTTGAAGAATGGAATTGATATT
1559-1640
FSTL5-203 ACACCAAAGCTTTCCAAACAACTCACGCTTCAAGCAAATGGCAGTGAGGTTCACATAAGCAATGTGCGCTATGAAGATACTG
S1R ACACCAAAGCTTTCCAAACAACTCACGCTTCAAGCAAATGGCAGTGAGGTTCACATAAGCAATGTGCGCTATGAAGATACTG
S1F ACACCAAAGCTTTCCAAACAACTCACGCTTCAAGCAAATGGCAGTGAGGTTCACATAAGCAATGTGCGCTATGAAGATACTG
S2R ACACCAAAGCTTTCCAAACAACTCACGCTTCAAGCAAATGGCAGTGAGGTTCACATAAGCAATGTGCGCTATGAAGATACTG
S2F ACACCAAAGCTTTCCAAACAACTCACGCTTCAAGCAAATGGCAGTGAGGTTCACATAAGCAATGTGCGCTATGAAGATACTG
S3R ACACCAAAGCTTTCCAAACAACTCACGCTTCAAGCAAATGGCAGTGAGGTTCACATAAGCAATGTGCGCTATGAAGATACTG
S3F ACACCAAAGCTTTCCAAACAACTCACGCTTCAAGCAAATGGCAGTGAGGTTCACATAAGCAATGTGCGCTATGAAGATACTG
1641-1722
exon 10
FSTL5-203 GAGCATACACTTGTATCGCAAAGAATGAAGCAGGAGTGGATGAAGACATCTCTTCTCTTTTTGTGGAAGACTCTGCTAGAAA
S1R GAGCATACACTTGTATCGCAAAGAATGAAGCAGGAGTGGATGAAGACATCTCTTCTCTTTTTGTGGAAGACTCTGCTAGAAA
S1F GAGCATACACTTGTATCGCAAAGAATGAAGCAGGAGTGGATGAAGACATCTCTTCTCTTTTTGTGGAAGACTCTGCTAGAAA
S2R GAGCATACACTTGTATCGCAAAGAATGAAGCAGGAGTGGATGAAGACATCTCTTCTCTTTTTGTGGAAGACTCTGCTAGAAA
S2F GAGCATACACTTGTATCGCAAAGAATGAAGCAGGAGTGGATGAAGACATCTCTTCTCTTTTTGTGGAAGACTCTGCTAGAAA
S3R GAGCATACACTTGTATCGCAAAGAATGAAGCAGGAGTGGATGAAGACATCTCTTCTCTTTTTGTGGAAGACTCTGCTAGAAA
S3F GAGCATACACTTGTATCGCAAAGAATGAAGCAGGAGTGGATGAAGACATCTCTTCTCTTTTTGTGGAAGACTCTGCTAGAAA
1723-1804
exon 11
FSTL5-203 GACCCGTCTGGGAATTGGGAACATGTTCTATGTTTTTTATGAAGATGGAATCAAAGTGATACAACCCATAGAATGTGAATTT
S1R GACCCGTCTGGGAATTGGGAACATGTTCTATGTTTTTTATGAAGATGGAATCAAAGTGATACAACCCATAGAATGTGAATTT
S1F GACCCGTCTGGGAATTGGGAACATGTTCTATGTTTTTTATGAAGATGGAATCAAAGTGATACAACCCATAGAATGTGAATTT
S2R GACCCGTCTGGGAATTGGGAACATGTTCTATGTTTTTTATGAAGATGGAATCAAAGTGATACAACCCATAGAATGTGAATTT
S2F GACCCGTCTGGGAATTGGGAACATGTTCTATGTTTTTTATGAAGATGGAATCAAAGTGATACAACCCATAGAATGTGAATTT
S3R GACCCGTCTGGGAATTGGGAACATGTTCTATGTTTTTTATGAAGATGGAATCAAAGTGATACAACCCATAGAATGTGAATTT
S3F GACCCGTCTGGGAATTGGGAACATGTTCTATGTTTTTTATGAAGATGGAATCAAAGTGATACAACCCATAGAATGTGAATTT
1805-1886
exon 12
FSTL5-203 CAGAGGCACATTAAGCCTAGTGAAAAGCTCCTTGGATTTCAGGATGAAGTCTGTCCCAAAGCTGAGG
S1R CAGAGGCACATTAAGCCTAGTGAAAAGCTCCTTGGATTTCAGGATGAAGTCTGTTCCCAAAGCTGAG
S1F CAGAGGCACATTAAGCCTAGTGAAAAGCTCCTTGGATTTCAGGATGAAGTCTGTCCCAAAGCTGAGG
S2R CAGAGGCACATTAAGCCTAGTGAAAAGCTCCTTGGATTTCAGGATGAAGTCT-TCCCAAAGCGAGGA
S2F CAGAGGCACATTAAGCCTAGTGAAAAGCTCCTTGGATTTCAGGATGAAGTCTGTCCCAAAGCTGAGG
S3R CAGAGGCACATTAAGCCTAGTGAAAAGCTCCTTGGATTTCAGGATGAAGTCTGTTCCCAAAGCGAGG
S3F CAGAGGCACATTAAGCCTAGTGAAAAGCTCCTTGGATTTCAGGATGAAGTCTGTCCCAAAGCTGAGG

B

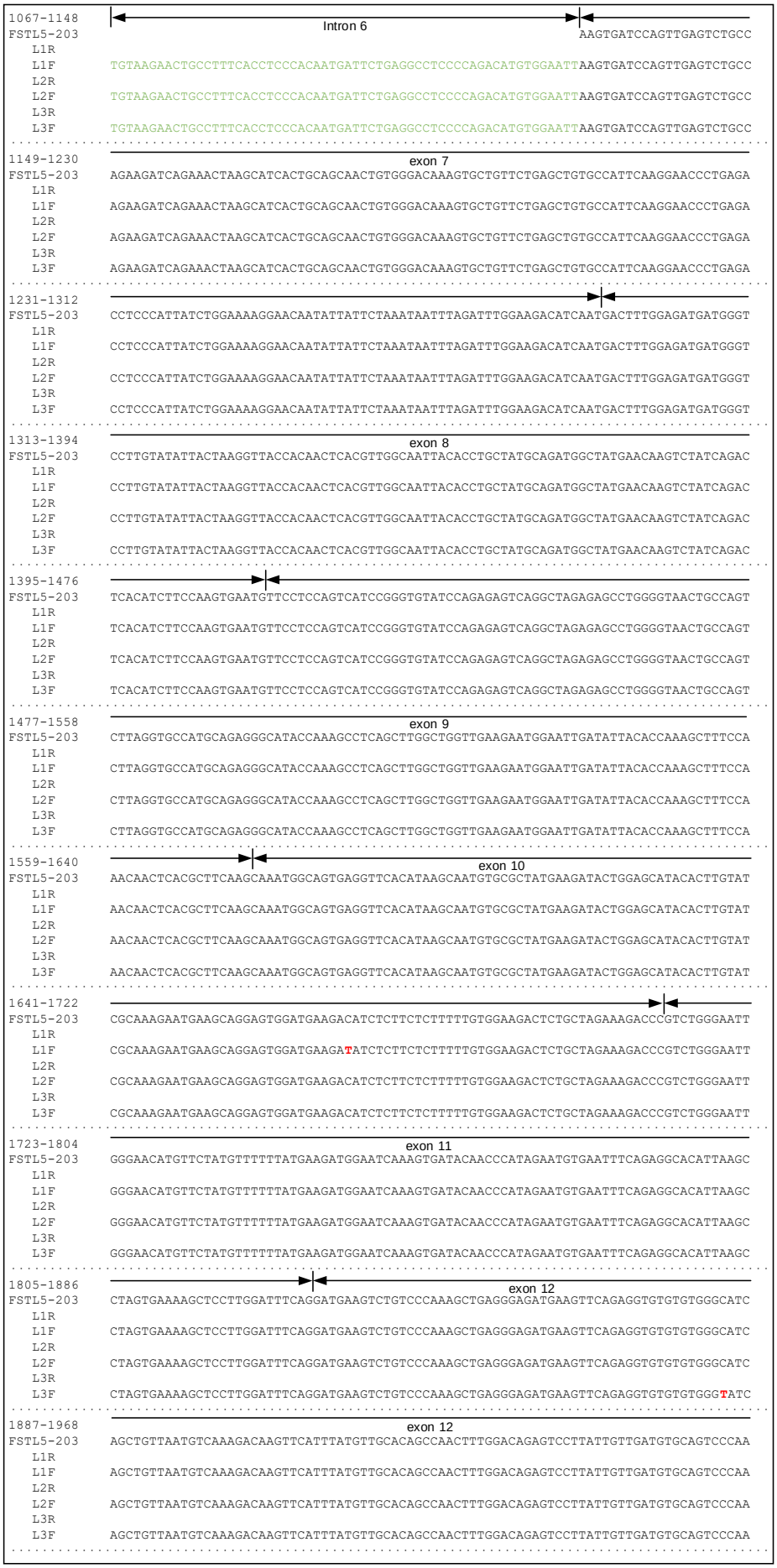
1067-1148
Intron 6
FSTL5-203 AAGTGATCCAGTTGAGTCTGCC
L1R
L1F TGTAAGAACTGCCTTTCACCTCCCACAATGATTCTGAGGCCTCCCCAGACATGTGGAATTAAGTGATCCAGTTGAGTCTGCC
L2R
L2F TGTAAGAACTGCCTTTCACCTCCCACAATGATTCTGAGGCCTCCCCAGACATGTGGAATTAAGTGATCCAGTTGAGTCTGCC
L3R
L3F TGTAAGAACTGCCTTTCACCTCCCACAATGATTCTGAGGCCTCCCCAGACATGTGGAATTAAGTGATCCAGTTGAGTCTGCC
1149-1230
exon 7
FSTL5-203 AGAAGATCAGAAACTAAGCATCACTGCAGCAACTGTGGGACAAAGTGCTGTTCTGAGCTGTGCCATTCAAGGAACCCTGAGA
L1R
L1F AGAAGATCAGAAACTAAGCATCACTGCAGCAACTGTGGGACAAAGTGCTGTTCTGAGCTGTGCCATTCAAGGAACCCTGAGA
L2R
L2F AGAAGATCAGAAACTAAGCATCACTGCAGCAACTGTGGGACAAAGTGCTGTTCTGAGCTGTGCCATTCAAGGAACCCTGAGA
L3R
L3F AGAAGATCAGAAACTAAGCATCACTGCAGCAACTGTGGGACAAAGTGCTGTTCTGAGCTGTGCCATTCAAGGAACCCTGAGA
1231-1312
FSTL5-203 CCTCCCATTATCTGGAAAAGGAACAATATTATTCTAAATAATTTAGATTTGGAAGACATCAATGACTTTGGAGATGATGGGT
L1R
L1F CCTCCCATTATCTGGAAAAGGAACAATATTATTCTAAATAATTTAGATTTGGAAGACATCAATGACTTTGGAGATGATGGGT
L2R
L2F CCTCCCATTATCTGGAAAAGGAACAATATTATTCTAAATAATTTAGATTTGGAAGACATCAATGACTTTGGAGATGATGGGT
L3R
L3F CCTCCCATTATCTGGAAAAGGAACAATATTATTCTAAATAATTTAGATTTGGAAGACATCAATGACTTTGGAGATGATGGGT
1313-1394
exon 8
FSTL5-203 CCTTGTATATTACTAAGGTTACCACAACTCACGTTGGCAATTACACCTGCTATGCAGATGGCTATGAACAAGTCTATCAGAC
L1R
L1F CCTTGTATATTACTAAGGTTACCACAACTCACGTTGGCAATTACACCTGCTATGCAGATGGCTATGAACAAGTCTATCAGAC
L2R
L2F CCTTGTATATTACTAAGGTTACCACAACTCACGTTGGCAATTACACCTGCTATGCAGATGGCTATGAACAAGTCTATCAGAC
L3R
L3F CCTTGTATATTACTAAGGTTACCACAACTCACGTTGGCAATTACACCTGCTATGCAGATGGCTATGAACAAGTCTATCAGAC
1395-1476
FSTL5-203 TCACATCTTCCAAGTGAATGTTCCTCCAGTCATCCGGGTGTATCCAGAGAGTCAGGCTAGAGAGCCTGGGGTAACTGCCAGT
L1R
L1F TCACATCTTCCAAGTGAATGTTCCTCCAGTCATCCGGGTGTATCCAGAGAGTCAGGCTAGAGAGCCTGGGGTAACTGCCAGT
L2R
L2F TCACATCTTCCAAGTGAATGTTCCTCCAGTCATCCGGGTGTATCCAGAGAGTCAGGCTAGAGAGCCTGGGGTAACTGCCAGT
L3R
L3F TCACATCTTCCAAGTGAATGTTCCTCCAGTCATCCGGGTGTATCCAGAGAGTCAGGCTAGAGAGCCTGGGGTAACTGCCAGT
1477-1558
exon 9
FSTL5-203 CTTAGGTGCCATGCAGAGGGCATACCAAAGCCTCAGCTTGGCTGGTTGAAGAATGGAATTGATATTACACCAAAGCTTTCCA
L1R
L1F CTTAGGTGCCATGCAGAGGGCATACCAAAGCCTCAGCTTGGCTGGTTGAAGAATGGAATTGATATTACACCAAAGCTTTCCA
L2R
L2F CTTAGGTGCCATGCAGAGGGCATACCAAAGCCTCAGCTTGGCTGGTTGAAGAATGGAATTGATATTACACCAAAGCTTTCCA
L3R
L3F CTTAGGTGCCATGCAGAGGGCATACCAAAGCCTCAGCTTGGCTGGTTGAAGAATGGAATTGATATTACACCAAAGCTTTCCA
1559-1640
exon 10
FSTL5-203 AACAACTCACGCTTCAAGCAAATGGCAGTGAGGTTCACATAAGCAATGTGCGCTATGAAGATACTGGAGCATACACTTGTAT
L1R
L1F AACAACTCACGCTTCAAGCAAATGGCAGTGAGGTTCACATAAGCAATGTGCGCTATGAAGATACTGGAGCATACACTTGTAT
L2R
L2F AACAACTCACGCTTCAAGCAAATGGCAGTGAGGTTCACATAAGCAATGTGCGCTATGAAGATACTGGAGCATACACTTGTAT
L3R
L3F AACAACTCACGCTTCAAGCAAATGGCAGTGAGGTTCACATAAGCAATGTGCGCTATGAAGATACTGGAGCATACACTTGTAT
1641-1722
FSTL5-203 CGCAAAGAATGAAGCAGGAGTGGATGAAGACATCTCTTCTCTTTTTGTGGAAGACTCTGCTAGAAAGACCCGTCTGGGAATT
L1R
L1F CGCAAAGAATGAAGCAGGAGTGGATGAAGATATCTCTTCTCTTTTTGTGGAAGACTCTGCTAGAAAGACCCGTCTGGGAATT
L2R
L2F CGCAAAGAATGAAGCAGGAGTGGATGAAGACATCTCTTCTCTTTTTGTGGAAGACTCTGCTAGAAAGACCCGTCTGGGAATT
L3R
L3F CGCAAAGAATGAAGCAGGAGTGGATGAAGACATCTCTTCTCTTTTTGTGGAAGACTCTGCTAGAAAGACCCGTCTGGGAATT
1723-1804
exon 11
FSTL5-203 GGGAACATGTTCTATGTTTTTTATGAAGATGGAATCAAAGTGATACAACCCATAGAATGTGAATTTCAGAGGCACATTAAGC
L1R
L1F GGGAACATGTTCTATGTTTTTTATGAAGATGGAATCAAAGTGATACAACCCATAGAATGTGAATTTCAGAGGCACATTAAGC
L2R
L2F GGGAACATGTTCTATGTTTTTTATGAAGATGGAATCAAAGTGATACAACCCATAGAATGTGAATTTCAGAGGCACATTAAGC
L3R
L3F GGGAACATGTTCTATGTTTTTTATGAAGATGGAATCAAAGTGATACAACCCATAGAATGTGAATTTCAGAGGCACATTAAGC
1805-1886
exon 12
FSTL5-203 CTAGTGAAAAGCTCCTTGGATTTCAGGATGAAGTCTGTCCCAAAGCTGAGGGAGATGAAGTTCAGAGGTGTGTGTGGGCATC
L1R
L1F CTAGTGAAAAGCTCCTTGGATTTCAGGATGAAGTCTGTCCCAAAGCTGAGGGAGATGAAGTTCAGAGGTGTGTGTGGGCATC
L2R
L2F CTAGTGAAAAGCTCCTTGGATTTCAGGATGAAGTCTGTCCCAAAGCTGAGGGAGATGAAGTTCAGAGGTGTGTGTGGGCATC
L3R
L3F CTAGTGAAAAGCTCCTTGGATTTCAGGATGAAGTCTGTCCCAAAGCTGAGGGAGATGAAGTTCAGAGGTGTGTGTGGGTATC
1887-1968
exon 12
FSTL5-203 AGCTGTTAATGTCAAAGACAAGTTCATTTATGTTGCACAGCCAACTTTGGACAGAGTCCTTATTGTTGATGTGCAGTCCCAA
L1R
L1F AGCTGTTAATGTCAAAGACAAGTTCATTTATGTTGCACAGCCAACTTTGGACAGAGTCCTTATTGTTGATGTGCAGTCCCAA
L2R
L2F AGCTGTTAATGTCAAAGACAAGTTCATTTATGTTGCACAGCCAACTTTGGACAGAGTCCTTATTGTTGATGTGCAGTCCCAA
L3R
L3F AGCTGTTAATGTCAAAGACAAGTTCATTTATGTTGCACAGCCAACTTTGGACAGAGTCCTTATTGTTGATGTGCAGTCCCAA

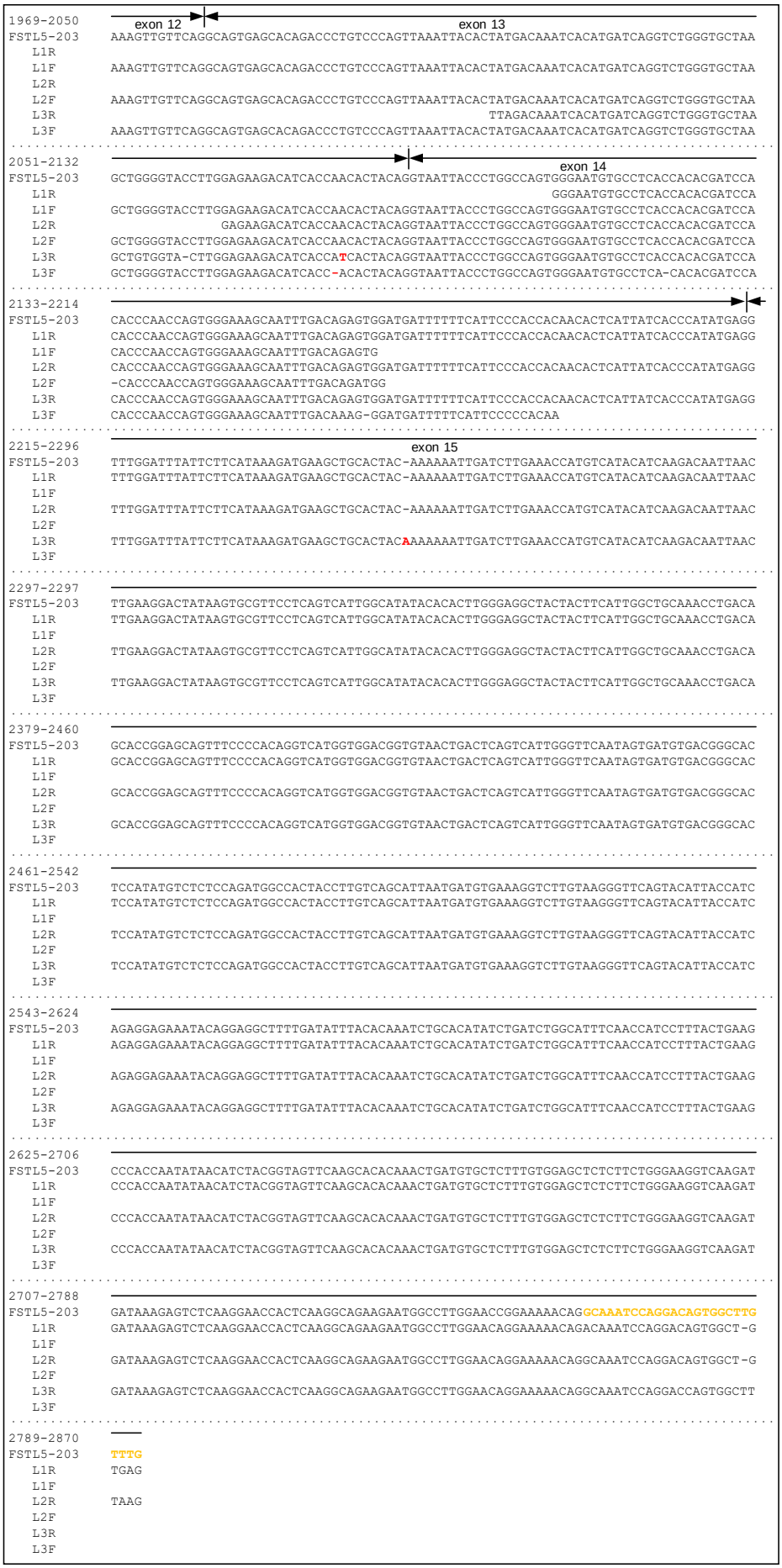
1969-2050
exon 12
exon 13
FSTL5-203 AAAGTTGTTCAGGCAGTGAGCACAGACCCTGTCCCAGTTAAATTACACTATGACAAATCACATGATCAGGTCTGGGTGCTAA
L1R
L1F AAAGTTGTTCAGGCAGTGAGCACAGACCCTGTCCCAGTTAAATTACACTATGACAAATCACATGATCAGGTCTGGGTGCTAA
L2R
L2F AAAGTTGTTCAGGCAGTGAGCACAGACCCTGTCCCAGTTAAATTACACTATGACAAATCACATGATCAGGTCTGGGTGCTAA
L3R TTAGACAAATCACATGATCAGGTCTGGGTGCTAA
L3F AAAGTTGTTCAGGCAGTGAGCACAGACCCTGTCCCAGTTAAATTACACTATGACAAATCACATGATCAGGTCTGGGTGCTAA
2051-2132
exon 14
FSTL5-203 GCTGGGGTACCTTGGAGAAGACATCACCAACACTACAGGTAATTACCCTGGCCAGTGGGAATGTGCCTCACCACACGATCCA
L1R GGGAATGTGCCTCACCACACGATCCA
L1F GCTGGGGTACCTTGGAGAAGACATCACCAACACTACAGGTAATTACCCTGGCCAGTGGGAATGTGCCTCACCACACGATCCA
L2R GAGAAGACATCACCAACACTACAGGTAATTACCCTGGCCAGTGGGAATGTGCCTCACCACACGATCCA
L2F GCTGGGGTACCTTGGAGAAGACATCACCAACACTACAGGTAATTACCCTGGCCAGTGGGAATGTGCCTCACCACACGATCCA
L3R GCTGTGGTA-CTTGGAGAAGACATCACCATCACTACAGGTAATTACCCTGGCCAGTGGGAATGTGCCTCACCACACGATCCA
L3F GCTGGGGTACCTTGGAGAAGACATCACC-ACACTACAGGTAATTACCCTGGCCAGTGGGAATGTGCCTCA-CACACGATCCA
2133-2214
FSTL5-203 CACCCAACCAGTGGGAAAGCAATTTGACAGAGTGGATGATTTTTTCATTCCCACCACAACACTCATTATCACCCATATGAGG
L1R CACCCAACCAGTGGGAAAGCAATTTGACAGAGTGGATGATTTTTTCATTCCCACCACAACACTCATTATCACCCATATGAGG
L1F CACCCAACCAGTGGGAAAGCAATTTGACAGAGTG
L2R CACCCAACCAGTGGGAAAGCAATTTGACAGAGTGGATGATTTTTTCATTCCCACCACAACACTCATTATCACCCATATGAGG
L2F -CACCCAACCAGTGGGAAAGCAATTTGACAGATGG
L3R CACCCAACCAGTGGGAAAGCAATTTGACAGAGTGGATGATTTTTTCATTCCCACCACAACACTCATTATCACCCATATGAGG
L3F CACCCAACCAGTGGGAAAGCAATTTGACAAAG-GGATGATTTTTCATTCCCCCACAA
2215-2296
exon 15
FSTL5-203 TTTGGATTTATTCTTCATAAAGATGAAGCTGCACTAC-AAAAAATTGATCTTGAAACCATGTCATACATCAAGACAATTAAC
L1R TTTGGATTTATTCTTCATAAAGATGAAGCTGCACTAC-AAAAAATTGATCTTGAAACCATGTCATACATCAAGACAATTAAC
L1F
L2R TTTGGATTTATTCTTCATAAAGATGAAGCTGCACTAC-AAAAAATTGATCTTGAAACCATGTCATACATCAAGACAATTAAC
L2F
L3R TTTGGATTTATTCTTCATAAAGATGAAGCTGCACTACAAAAAAATTGATCTTGAAACCATGTCATACATCAAGACAATTAAC
L3F
2297-2297
FSTL5-203 TTGAAGGACTATAAGTGCGTTCCTCAGTCATTGGCATATACACACTTGGGAGGCTACTACTTCATTGGCTGCAAACCTGACA
L1R TTGAAGGACTATAAGTGCGTTCCTCAGTCATTGGCATATACACACTTGGGAGGCTACTACTTCATTGGCTGCAAACCTGACA
L1F
L2R TTGAAGGACTATAAGTGCGTTCCTCAGTCATTGGCATATACACACTTGGGAGGCTACTACTTCATTGGCTGCAAACCTGACA
L2F
L3R TTGAAGGACTATAAGTGCGTTCCTCAGTCATTGGCATATACACACTTGGGAGGCTACTACTTCATTGGCTGCAAACCTGACA
L3F
2379-2460
FSTL5-203 GCACCGGAGCAGTTTCCCCACAGGTCATGGTGGACGGTGTAACTGACTCAGTCATTGGGTTCAATAGTGATGTGACGGGCAC
L1R GCACCGGAGCAGTTTCCCCACAGGTCATGGTGGACGGTGTAACTGACTCAGTCATTGGGTTCAATAGTGATGTGACGGGCAC
L1F
L2R GCACCGGAGCAGTTTCCCCACAGGTCATGGTGGACGGTGTAACTGACTCAGTCATTGGGTTCAATAGTGATGTGACGGGCAC
L2F
L3R GCACCGGAGCAGTTTCCCCACAGGTCATGGTGGACGGTGTAACTGACTCAGTCATTGGGTTCAATAGTGATGTGACGGGCAC
L3F
2461-2542
FSTL5-203 TCCATATGTCTCTCCAGATGGCCACTACCTTGTCAGCATTAATGATGTGAAAGGTCTTGTAAGGGTTCAGTACATTACCATC
L1R TCCATATGTCTCTCCAGATGGCCACTACCTTGTCAGCATTAATGATGTGAAAGGTCTTGTAAGGGTTCAGTACATTACCATC
L1F
L2R TCCATATGTCTCTCCAGATGGCCACTACCTTGTCAGCATTAATGATGTGAAAGGTCTTGTAAGGGTTCAGTACATTACCATC
L2F
L3R TCCATATGTCTCTCCAGATGGCCACTACCTTGTCAGCATTAATGATGTGAAAGGTCTTGTAAGGGTTCAGTACATTACCATC
L3F
2543-2624
FSTL5-203 AGAGGAGAAATACAGGAGGCTTTTGATATTTACACAAATCTGCACATATCTGATCTGGCATTTCAACCATCCTTTACTGAAG
L1R AGAGGAGAAATACAGGAGGCTTTTGATATTTACACAAATCTGCACATATCTGATCTGGCATTTCAACCATCCTTTACTGAAG
L1F
L2R AGAGGAGAAATACAGGAGGCTTTTGATATTTACACAAATCTGCACATATCTGATCTGGCATTTCAACCATCCTTTACTGAAG
L2F
L3R AGAGGAGAAATACAGGAGGCTTTTGATATTTACACAAATCTGCACATATCTGATCTGGCATTTCAACCATCCTTTACTGAAG
L3F
2625-2706
FSTL5-203 CCCACCAATATAACATCTACGGTAGTTCAAGCACACAAACTGATGTGCTCTTTGTGGAGCTCTCTTCTGGGAAGGTCAAGAT
L1R CCCACCAATATAACATCTACGGTAGTTCAAGCACACAAACTGATGTGCTCTTTGTGGAGCTCTCTTCTGGGAAGGTCAAGAT
L1F
L2R CCCACCAATATAACATCTACGGTAGTTCAAGCACACAAACTGATGTGCTCTTTGTGGAGCTCTCTTCTGGGAAGGTCAAGAT
L2F
L3R CCCACCAATATAACATCTACGGTAGTTCAAGCACACAAACTGATGTGCTCTTTGTGGAGCTCTCTTCTGGGAAGGTCAAGAT
L3F
2707-2788
FSTL5-203 GATAAAGAGTCTCAAGGAACCACTCAAGGCAGAAGAATGGCCTTGGAACCGGAAAAACAGGCAAATCCAGGACAGTGGCTTG
L1R GATAAAGAGTCTCAAGGAACCACTCAAGGCAGAAGAATGGCCTTGGAACAGGAAAAACAGACAAATCCAGGACAGTGGCT-G
L1F
L2R GATAAAGAGTCTCAAGGAACCACTCAAGGCAGAAGAATGGCCTTGGAACAGGAAAAACAGGCAAATCCAGGACAGTGGCT-G
L2F
L3R GATAAAGAGTCTCAAGGAACCACTCAAGGCAGAAGAATGGCCTTGGAACAGGAAAAACAGGCAAATCCAGGACCAGTGGCTT
L3F
2789-2870
FSTL5-203 TTTG
L1R TGAG
L1F
L2R TAAG
L2F
L3R
L3F

Appendix 3: Comparison of different antibodies' performances. INA-6 cells were treated with 10% HS, 0.1% BSA, 10% HS with PTI, and 0.1% BSA with PTI (same medium order displayed on the four lanes of each membrane) for 4 hours. The cells were then used for western blot with FSTL5 antibody A, B, C, D, E, and F. The figure shows the results of one experiment.

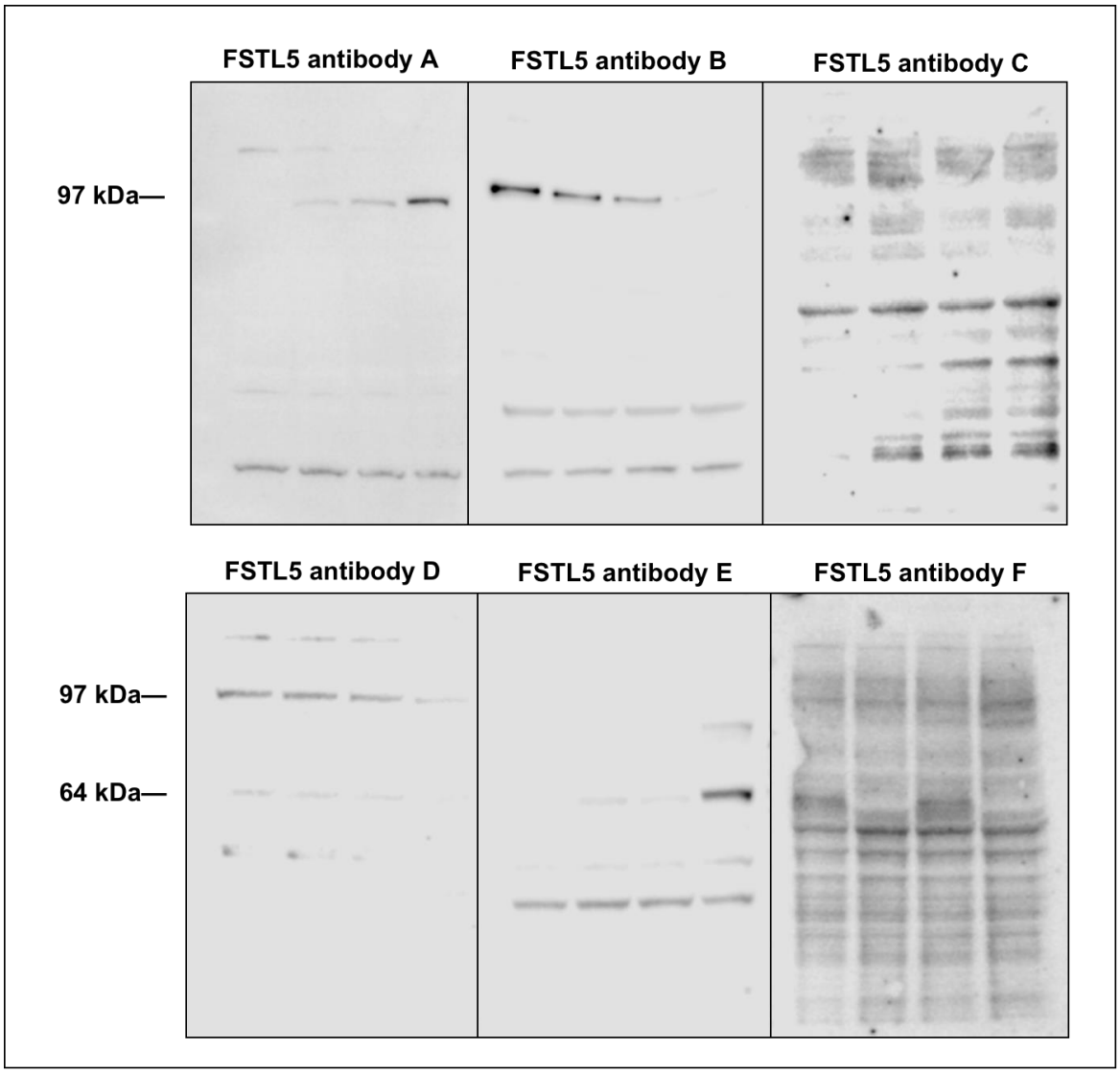

Appendix 4: Validation of antibodies with FSTL5 KO cells. FSTL5 exon 5 KO, FSTL5 exon 8 KO, and FSTL5 WT control cells were incubated in 10% HS or 0.1% BSA with/without PTI for 4 hours. The cells were then used for western blot with FSTL5 antibody A, B, and E. GAPDH antibody was used as the loading control. The figure shows one of the two irreproducible results.

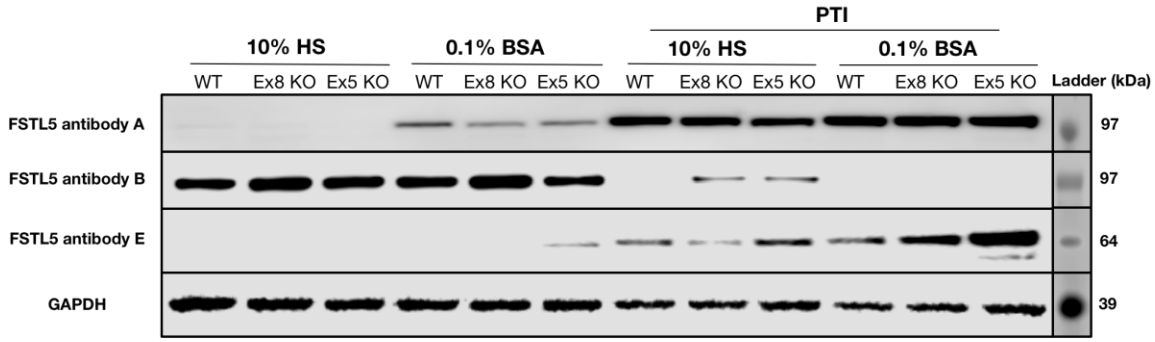

Appendix 5: Expression of FSTL5 across eight HMCLs by RNA-seq. The RNA-seq results obtained from our laboratory were normalized to TPM (Transcripts Per Kilobase Million) which was then log-transformed and displayed on the figure. The log-transformed values below zero indicate low to no expression of FSTL5.

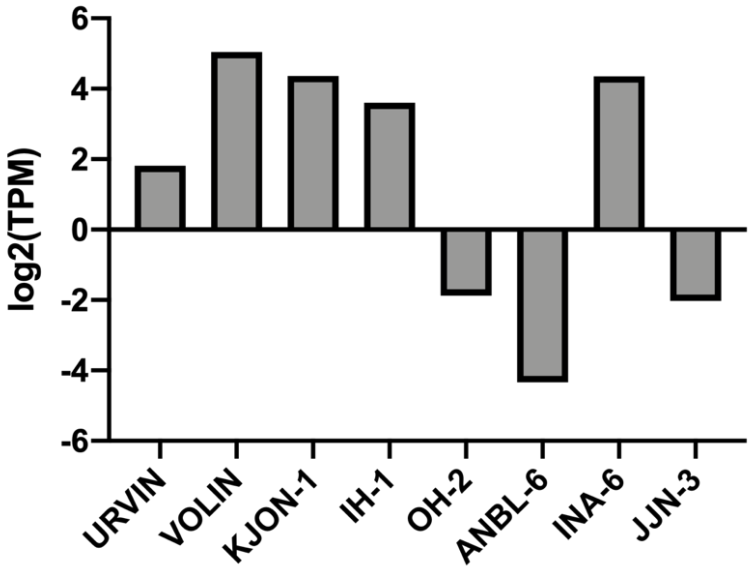

Appendix 6: Sequence alignments with FSTL5 transcript variants. Sequencing results of FSTL5 short primer products and long primer products were aligned with FSTL5-201 (A) and FSTL5-202 (B), respectively. The exon numbers were marked within each template. The gray areas represent sequences that are the same as the template and the red areas are mismatched sequences.

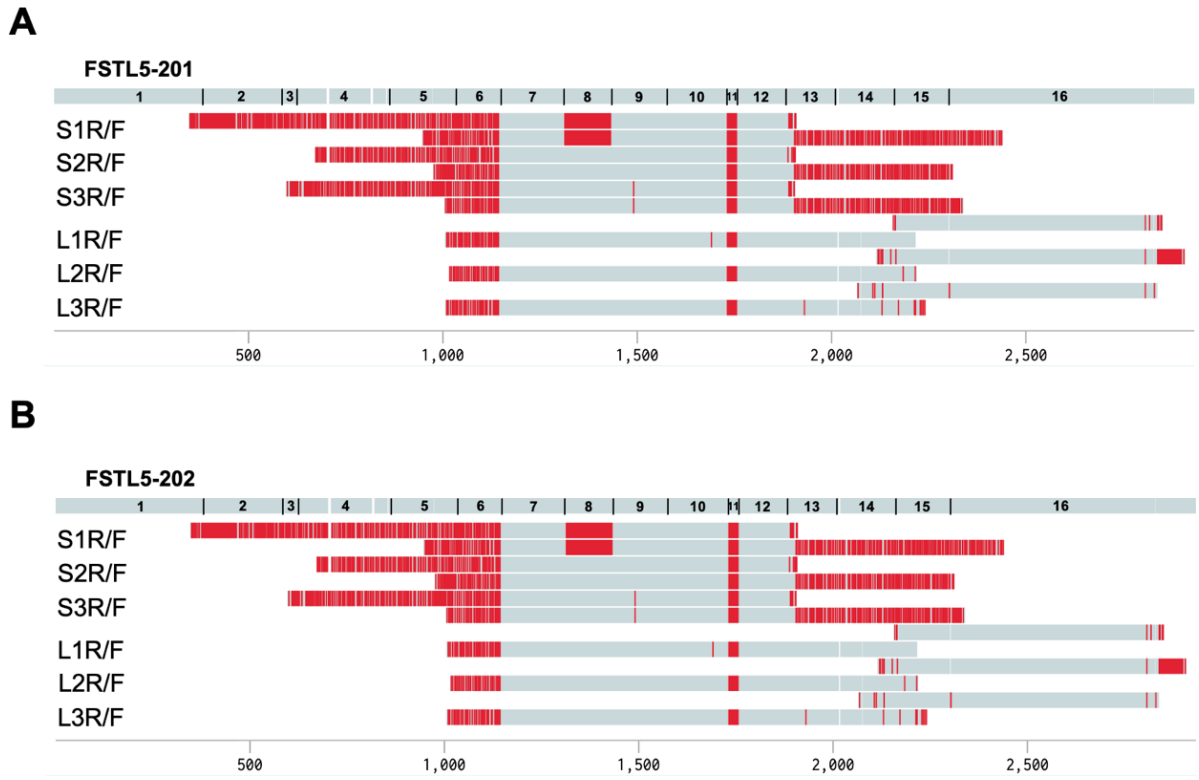

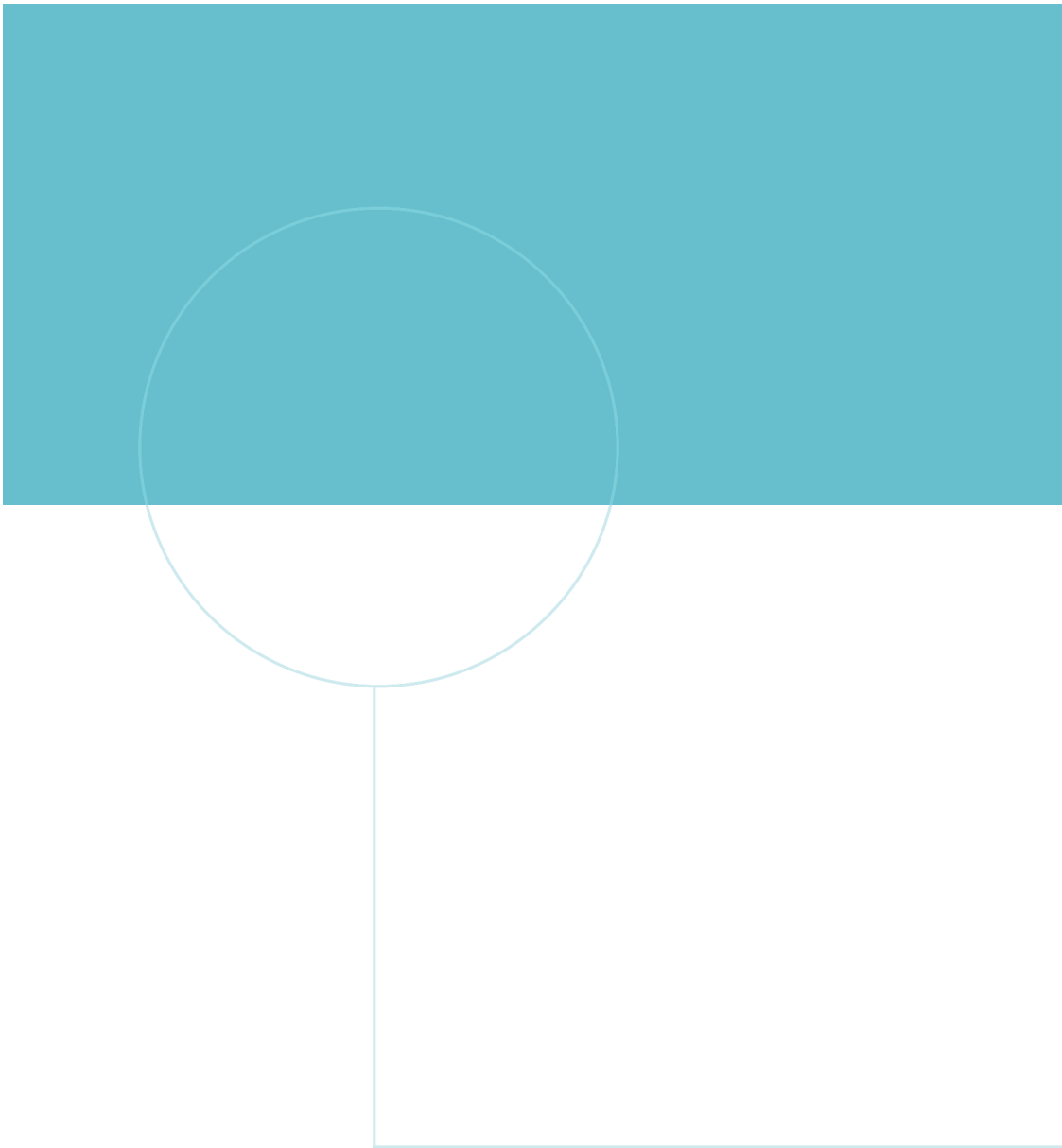

NTNU

Norwegian University of
Science and Technology